# RESEARCH ACTIVITIES IV
# Department of Molecular Assemblies

## IV-A Optical Study of Charge Ordering States in Organic Conductors

In the organic charge-transfer salts, the charge carriers in organic crystal is located at the boundary between localized and extended (delocalized) states, mainly because the interatomic distances between the neighboring molecules are much longer than the bond length within the molecule. Therefore, charge ordering (CO) originated from the localization of the charge carriers is widely found in organic conductors through the phase transition. Recently, CO has been found in several organic conductors, and the electronic phase diagrams of typical organic conductors are re-considered taking CO into account. The CO state is drawing attention, first because a CO phase is neighbored on a superconducting phase, wherein a new type of pairing mechanism for superconductivity is theoretically predicted, second because some compounds in a CO phase shows ferroelectric property. To detect CO states, we employ infrared and Raman spectroscopy. Some molecules have charge-sensitive intramolecular vibrational modes, the frequency of which shifts proportional to the molecular charge (oxidation state of molecule). The Raman and infrared spectra change dramatically at the CO phase-transition temperature, since CO is accompanied by an inhomogeneous distribution of molecular charge. The goal of this study is (1) the understanding of the unusual electronic state of the conducting phase above the CO phase transition, (2) the investigation of the optical properties related to the ferroelectric CO phase, and (3) the characterization of the insulating electronic state near the superconducting phase.

### IV-A-1 Examination of the Charge-Sensitive Vibrational Modes in ET Molecule

**YAMAMOTO, Takashi; YAKUSHI, Kyuya; URUICHI, Mikio; YAMAMOTO, Kaoru; KAWAMOTO, Atsushi[1]; TANIGUCHI, Hiromi[2]**
*([1]Hokkaido Univ.; [2]Saitama Univ.)*

[*J. Phys. Chem. B* **109**, 15226 (2005)]

We re-investigated the two C=C stretching modes of the five-member rings of ET [ET = bis(ethylenedithio) tetrathiafulvalene], namely, $\nu_2$ (in-phase mode) and $\nu_{27}$ (out-of-phase mode). The frequency of the $\nu_{27}$ mode of $ET^+$ was corrected to be ~1400 $cm^{-1}$, which was identified from the polarized infrared reflectance spectra of $(ET)(ClO_4)$, $(ET)(AuBr_2Cl_2)$ and the deuterium- or $^{13}C$-substituted compounds of $(ET)(AuBr_2Cl_2)$. It was clarified from DFT calculations that the frequency of the $\nu_{27}$ mode of the flat $ET^0$ molecule was significantly different from that of the boat-shaped $ET^0$ molecule. We obtained the linear relationship between the frequency and the charge on the molecule, $\rho$, for the flat ET molecule, which was shown to be $\nu_{27}(\rho) = 1398 + 140(1-\rho)$ $cm^{-1}$. The frequency shift due to oxidation is remarkably larger than reported in previous studies. The fractional charges of several ET salts in a charge-ordered state can be successfully estimated by applying this relationship. Therefore, the $\nu_{27}$ mode is an efficient probe to detect $\rho$ in the charge-transfer salts of ET. Similarly, the linear relationship for the $\nu_2$ mode was obtained as $\nu_2(\rho) = 1447 + 120(1-\rho)$. This relationship was successfully applied to the charge-poor molecule of $\theta$-type ET salts in the charge-ordered state, but could not be applied to the charge-rich molecule. This discrepancy was semi-quantitatively explained by the hybridization between the $\nu_2$ and $\nu_3$ modes.

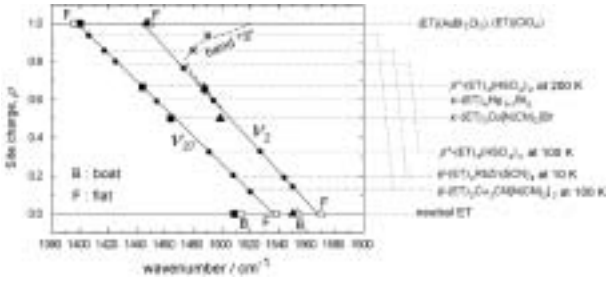


**Figure 1.** Frequencies of the $\nu_{27}$ and $\nu_2$ modes plotted as a function of the charge, $\rho$, on the ET molecule. Solid squares and solid triangles denote the experimental data, and open squares and open triangles denote the calculation data. The straight lines show the linear relationships between the frequencies and $\rho$, deduced from least-squares fitting. The $\rho$ value of the ET salts is inversely estimated from the linear relation and the data points thus obtained are indicated by solid circles. The broken line shows the $\rho$ dependence of the band "3", and × denotes the frequencies of the *A*-symmetry mode of the $\theta$-type ET salts.

### IV-A-2 Infrared and Raman Studies of $\theta$-(BEDT-TTF)$_2$CsZn(SCN)$_4$: Comparison with the Frozen State of $\theta$-(BEDT-TTF)$_2$RbZn(SCN)$_4$

**SUZUKI, Kenji[1]; YAMAMOTO, Kaoru; YAKUSHI, Kyuya; KAWAMOTO, Atsushi[2]**
*([1]SOKENDAI; [2]Hokkaido Univ.)*

[*J. Phys. Soc. Jpn.* **74**, 2631–2639 (2005)]

We present the optical conductivity and Raman spectra of $\theta$-(BEDT-TTF)$_2$CsZn(SCN)$_4$. The vibrational and vibronic bands in the 1200–1600 $cm^{-1}$ region was assigned with the aid of the $^{13}C$-substituted compound. The nearly uniform charge distribution was found in a

whole temperature range from 300 K to 6 K. However, the space group symmetry *I222* is locally broken already at room temperature. The broken symmetry suggests the resemblance to the high-temperature phase and frozen state of θ-(BEDT-TTF)$_2$RbZn(SCN)$_4$, which consists of short-range ordered charge-ordering domains. The amplitude in the charge-ordering domain of θ-(BEDT-TTF)$_2$CsZn(SCN)$_4$ is extremely small in a whole temperature range. At room temperature, hydrostatic pressure narrows the bandwidth of θ-(BEDT-TTF)$_2$CsZn(SCN)$_4$ to enlarge the amplitude in short-ranged ordered domains. The long-range ordered charge ordering in θ-(BEDT-TTF)$_2$CsZn(SCN)$_4$ was found at 10 K under the hydrostatic pressure of 2.5 GPa.

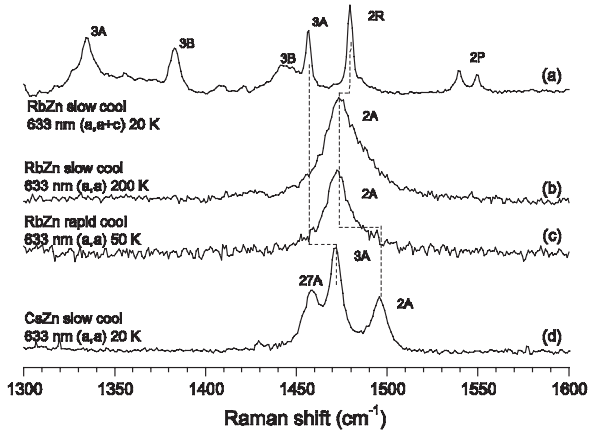


**Figure 1.** Comparison of the Raman spectra excited by 633 nm laser of slowly cooled RbZn measured at (a) 20 K (below $T_{CO}$) and (b) 200 K (above $T_{CO}$), (c) rapidly cooled RbZn measured at 50 K, and (d) slowly cooled CsZn measured at 20 K. $\nu_{2P}$ and $\nu_{2R}$ denote the $\nu_2$ modes at charge-poor ($\rho = 0.2$) site and charge-rich ($\rho = 0.8$) site, respectively.

### IV-A-3 Robust Superconducting State in the Low-Quasiparticle-Density Organic Metals β”-(BEDT-TTF)$_4$[(H$_3$O)*M*(C$_2$O$_4$)$_3$]·*Y*: Superconductivity due to Proximity to a Charge-Ordered State

**BANGURA, A. F.[1]; COLDEA, A. I.[1]; SINGLETON, J.[2]; ARDAVAN, A.[1]; AKUTSU-SATO, A.[3]; AKUTSU, H.[3]; TURNER, S. S.[3]; DAY, P.[3]; YAMAMOTO, Takashi; YAKUSHI, Kyuya**
*([1]Oxford Univ.; [2]Los Alamos Natl. Lab.; [3]Royal Inst. GB)*

[*Phys. Rev. B* **72**, 014543 (13 pages) (2005)]

We report magneto-transport measurements on the quasi-two-dimensional charge-transfer salts β”-(BEDT-TTF)$_4$[(H$_3$O)*M*(C$_2$O$_4$)$_3$]·*Y*, with *Y* = C$_6$H$_5$NO and C$_6$H$_5$CN using magnetic fields of up to 45 T and temperature down to 0.5 K. A surprisingly robust superconducting state with an in-plane upper critical field $B_{c2\|} \approx 33$ T, comparable to the highest critical field of any BEDT-TTF superconductor, and critical temperature $T_c \approx 7$ K is observed when *M* = Ga and *Y* = C$_6$H$_5$NO$_2$. The presence of magnetic *M* ions reduces the in-plane upper critical field to ≈18 T for *M* = Cr and *Y* = C$_6$H$_5$NO$_2$ and *M* = Fe and *Y* = C$_6$H$_5$CN. Prominent superconducting salts posses Fermi surfaces with one or two small quasi-two-dimensional pockets, their total area comprising ≤6% of the room-temperature Brillouin zone; the quasiparticle effective masses were found to be enhanced when the ion *M* was magnetic (Fe or Cr). The low effective masses and quasiparticle densities, and the systematic variation of the properties of the β”-(BEDT-TTF)$_4$[(H$_3$O)*M*(C$_2$O$_4$)$_3$]·*Y* salts with unit-cell volume points to the possibility of a superconducting ground state with a charge-fluctuation-mediated superconductivity mechanism such as that proposed by Merino and McKenzie [*Phys. Rev. Lett.* **87**, 237002 (2001)] rather than the spin-fluctuation mechanism appropriate for the κ-(BEDT-TTF)$_2$X salts.

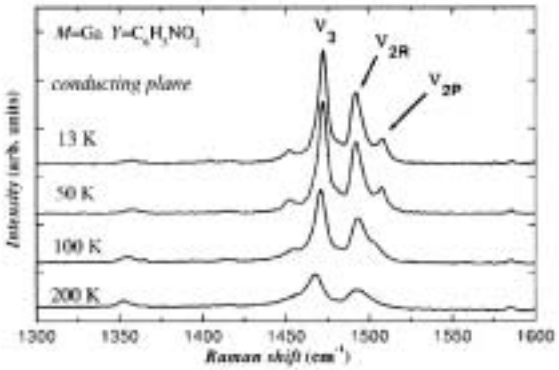


**Figure 1.** Raman spectra of β”-(BEDT-TTF)$_4$[(H$_3$O)Ga(C$_2$O$_4$)$_3$]·C$_6$H$_5$NO$_2$ taken at fixed temperature in the range 13 ≤ *T* ≤ 200 K. Note that the charge-sensitive $\nu_2$ band shows a clear splitting, which suggests the CO state below 50 K in this compound.

### IV-A-4 Influence of the Cooling Rate on Low-Temperature Raman and Infrared-Reflection Spectra of Partially Deuterated κ-(BEDT-TTF)$_2$Cu(N(CN)$_2$)Br

**MAKSIMUK, M.; YAKUSHI, Kyuya; TANIGUCHI, H.[1]; KANODA, Kazushi[1]; KAWAMOTO, Atsushi[2]**
*([1]Univ. Tokyo; [2]Hokkaido Univ.)*

[*Synth. Met.* **149**, 13–18 (2005)]

Raman and infrared-reflection spectra of κ-(BEDT-TTF)$_2$Cu(N(CN)$_2$)Br and its deuterated and partially deuterated analogues were measured at temperatures between 5 and 300 K and cooling rates from 1 to 20 K/min. It was found that, in partially deuterated samples, the interdimer electron-molecular vibration splitting of $\nu_3$ mode in Raman spectra, and linewidths of some phonon peaks both in Raman and infrared spectra depend on the cooling rate. These observations were explained by disorder-related effects.

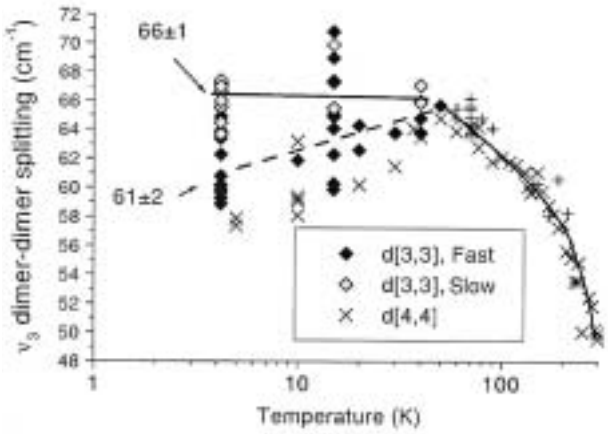


**Figure 1.** Temperature dependence of the dimer-dimer EMV (electron-molecular vibration) splitting of $\nu_3$ for d(3,3) after "slow" cooling (◇), "fast" cooling (◆), and above 50 K (crosses, +). The results for d(4,4) are also shown (crosses, ×). Lines are guide to the eye.

### IV-A-5 Optical Second Harmonic Generation in a Charge-Ordered Organic Conductor α-(BEDT-TTF)$_2$I$_3$

**YAMAMOTO, Kaoru; BOYKO, Sergiy; YAKUSHI, Kyuya; OKABE, Chie; NISHI, Nobuyuki; KASHIWAZAKI, Akimitsu[1]; HIRAMATSU, Fukiko[1]; IWAI, Shinichiro[1]**
*([1]Tohoku Univ.)*

Charge ordering (CO) in highly correlated CT complexes induces large modulation in the charge distribution. Since the modulation causes strong local polarization, it is suggested that such a polar state may show special features in dielectric properties, as ionic crystals do. In the present study, we investigated the nonlinear optical property of the title compound by means of the observation of second-harmonic generation (SHG). Near-IR ultra-short laser pulses were irradiated to a filmy single crystal as the excitation light, and the generated SH signal was detected in a transmission geometry.

It is known that this compound transforms from a semiconductor to an insulator at $T_{CO}$ (135 K) due to CO. As shown in (Figure 1), the SH signal emerges below $T_{CO}$, indicating that the inversion symmetry, existing at high temperatures, is broken by the spontaneous polarization induced by CO below $T_{CO}$. The prominent feature of the highly correlated system is in the competition of several electronic phases. Therefore, understanding of the mechanism of CO and then finding the way to connect it with the optical nonlinearity discovered here are important to explore the potential application of the correlated materials as a unique nonlinear optical media.

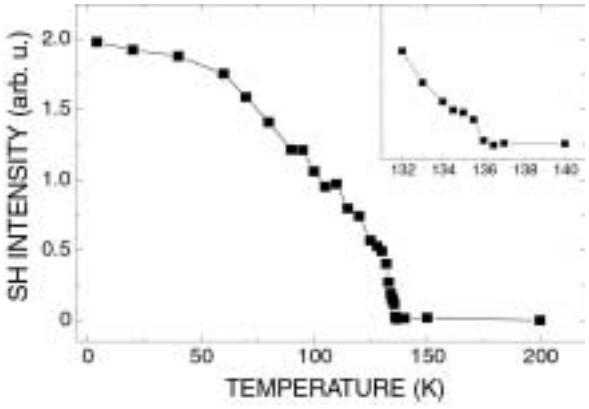


**Figure 1.** Temperature dependence of the intensity of second harmonic light from α-(BEDT-TTF)$_2$I$_3$. Inset shows the close-up of the data around $T_{CO}$.

### IV-A-6 Correlation between Structural Instabilities and Raman Shift and Width in β-(ET)$_2$I$_3$ and κ-(ET)$_2$Cu[N(CN)$_2$]I

**DROZDOVA, Olga; TANATAR, Makariy[1]; YAKUSHI, Kyuya; KUSHCH, N. D.[1]**
*([1]Inst. Problems Chem. Phys., RAS)*

Motivation of this study is to test the temperature dependence (Raman shift and width) of some selected intramolecular vibrations under the influence of both structural and electronic anomalies, in order to find a sensitive and reliable method to distinguish the nature clearly between such anomalies. For this purpose, we measured simultaneously the C=C modes of the ET molecule ($\nu_2$ and $\nu_3$, these are sensitive to ET geometry and local charge, as well as transfer integral), and CN mode of the polymeric anion (sensitive to structural effects only). Here we report the results obtained on the titled compounds because of possibility to directly compare the data with the published low-temperature structural studies.

(a) **β-(ET)$_2$I$_3$**: Anomalies in the Raman shift of $\nu_2$ were found at 100 and 170 K, where superstructures are known to appear.[1)] No abnormality was observed in the Raman shift of $\nu_3$ nor in the line width of the modes of $\nu_2$ and $\nu_3$.

(b) **κ-(ET)$_2$Cu[N(CN)$_2$]I**: Discontinuous jumps in the Raman shift (clear deviations from $T^2$ behavior) of both $\nu_2$ and $\nu_3$ ($A_g$), as well as ν(CN) were found at 155 and 220 K. These are characteristic temperatures where $0.5c^*$ and $0.38c^*$ superstructures are formed.[2)] In addition, a rapid increase in Raman shift of $\nu_2$ was observed below 45 K. On the other hand, $\nu_2$ ($B_{2g}$) showed approximately linear temperature dependence of an opposite sign, with a change of slope at 50 K. Further studies of κ-(ET)$_2$X compounds will be performed and compared with other physical properties.

**References**

1) T. Ishiguro, K. Yamaji, and G. Saito, *Organic Superconductors*, Springer 1998, and references therein.
2) M. A. Tanatar, V. S. Yefanov, S. Kagoshima, E. Ohmichi, T. Osada, N. D. Kushch and E. B. Yagubskii, *Phys. Rev. Lett.* submitted.

## IV-A-7 Inhomogeneous Charge Distribution in $(EDO\text{-}TTF)_2X$ (X = $ReO_4$ and $GaCl_4$)

**DROZDOVA, Olga; YAKUSHI, Kyuya; URUICHI, Mikio; OTA, Akira[1]; YAMOCHI, Hideki[1]; SAITO, Gunzi[1]**
*([1]Kyoto Univ.)*

Recently synthesized organic conductors $(EDO\text{-}TTF)_2X$ (where X = $ReO_4$ and $GaCl_4$) have quasi-one-dimensional (Q1D) crystal structure formed by two differently packed columns (A and B) of EDO-TTF alternated with chains of inorganic anion. Each column involves non-equivalent EDO-TTF molecules A1, A2, B1, and B2. The infrared spectra showed a phase transition at $T^*$ = 125 K, where the Drude contribution disappeared, an optical gap opened, and a strong vibronic bands emerged. On the other hand, the Raman spectra were insensitive to $T^*$, and showed no essential change in the whole temperature region 300–4.2 K. The Raman-active C=C stretching vibrations of EDO-TTF, sensitive to the molecular charge, were split into several components (Figure 1). These were interpreted as an inhomogeneous charge distribution on the four sites in the unit cell. From the Raman shift frequencies, the respective site charge differences were found as A1 – A2 = 0.25*e*, and B1 – B2 = 0.1*e*. Charge localization was suggested as a driving force of the phase transition at 125 K.

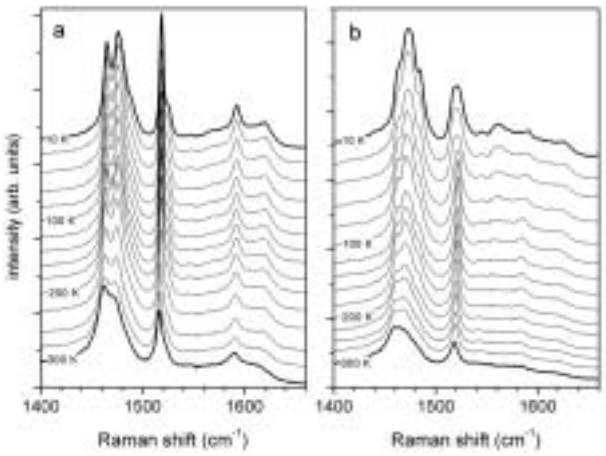


**Figure 1.** Temperature dependence of the Raman spectra of (a) $(EDO\text{-}TTF)_2ReO_4$ and (b) $(EDO\text{-}TTF)_2GaCl_4$.

## IV-A-8 Re-Examination of the Site Charge Difference in $TEA(TCNQ)_2$

**DROZDOVA, Olga; YAKUSHI, Kyuya**

In 1/4-filled organic charge transfer salts (CTS) the charge ordered (CO) state is classified into $4k_F$(0101) and $2k_F$(0110) waves. The latter is further divided into $2k_F$ BCDW-I (○‥○=●—●=○‥○ ) and $2k_F$ BCDW-II (○‥○ —●=●—○‥○ ), where the open circle has the charge of (1–Δ*q*)/2 and that at the solid circle has the charge of (1+Δ*q*)/2. We have recently analyzed the $2k_F$ BCDW-II state in $(EDO\text{-}TTF)_2X$ (X = $PF_6$, $AsF_6$).[1)] $TEA(TCNQ)_2$ is regarded as a typical representative compound for $2k_F$ BCDW-I based on the x-ray crystal structure analysis. We analyzed the site charge distribution using vibrational analysis and determined Δ*q*. The Raman-active (gerade) modes of TCNQ were perturbed by *emv* coupling. Therefore we employed the IR-active (ungerade) modes. $Cs_2(TCNQ)_3$ compound was used as a reference. The results obtained at 300 K and 6 K are summarized in the Table 1.

**Table 1.** Estimation of the difference in site charge, Δ*q*.

| TCNQ Mode | shift (per 1*e*) Δν cm$^{-1}$ | $Cs_2TCNQ_3$ obs. Δν cm$^{-1}$ | $Cs_2TCNQ_3$ charge difference Δ*q* | $TEA(TCNQ)_2$ 300 K Δν cm$^{-1}$ | 300 K Δ*q* | 6 K Δν cm$^{-1}$ | 6 K Δ*q* |
|---|---|---|---|---|---|---|---|
| $b_{2u}\nu_{34}$ C=C | 36 | 30 | 0.83 | 18 | 0.50 | 20 | 0.56 |
| $b_{2u}\nu_{33}$ C≡N | 75 | 50 | 0.67 | 44 | 0.59 | 47 | 0.63 |
| $b_{1u}\nu_{19}$ C≡N | 47 | 44 | 0.94 | 34 | 0.72 | 37 | 0.79 |
| averaged site charge | | | 0.78 | | 0.61 | | 0.66 |

**Reference**
1) O. Drozdova, K. Yakushi, K. Yamamoto, A. Ota, H. Yamochi, G. Saito, H. Tashiro and D. B. Tanner, *Phys. Rev. B* **70**, 075107 (2004).

## IV-A-9 Spectroscopic Evidence for the Monovalent-to-Divalent Phase Transition of Biferrocenium $(F_1TCNQ)_3$

**URUICHI, Mikio; YAKUSHI, Kyuya; MOCHIDA, Tomoyuki[1]**
*([1]Toho Univ.)*

[*J. Low Temp. Phys.* submitted]

The ionic crystal $D^+A_3^-$ (D = dineopentylbiferrocene and A = $F_1TCNQ$) undergoes a first-order phase transition, in which second ionization occurs to form a doubly ionized state, $D^{2+}A_3^{2-}$.[1)] As shown in the left panel of Figure 1, we found a dramatic change in the optical transition in the near-infrared region. This optical transition is interpreted as the charge-transfer excitation within the $F_1TCNQ$ trimer. We simulated the optical transition employing a trimer model. First, the transfer integral and site energy within the $F_1TCNQ$ trimer, $A^{3-}$, were estimated to reproduce the spectrum (oscillator strength and peak position) of 290 K. The site energy is introduced to take effectively the intra- and inter-trimer Coulomb interaction energy into account. Using the parameters thus obtained, the spectrum of $A_3^{2-}$ is simulated. As shown in the right panel of Figure 1, the change of this optical transition is quantitatively reproduced by the trimer model, in which the valence of the trimer changes from $A_3^-$ to $A_3^{2-}$. This result strongly supports the valence change character of this phase transition.

**Reference**
1) T. Mochida, K. Takazawa, M. Takahashi, M. Takeda, Y. Nishio, M. Sato, K. Kajita, H. Mori, M. M. Matsushita and T. Sugawara, *J. Phys. Soc. Jpn.* **74**, 2214 (2005).

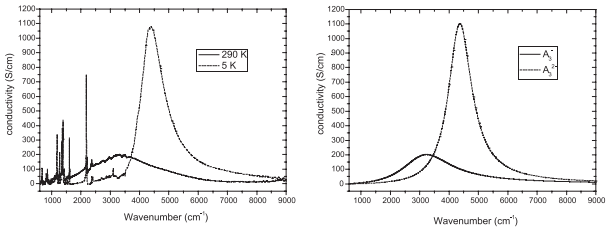


**Figure 1.** Optical conductivity spectra at 290 K and 5 K (left panel), and the Simulation based on a trimer model (right panel).

## IV-A-10 Phase Separation in the Monovalent-to-Divalent Phase Transition of Biferrocenium-$(F_1TCNQ)_3$

**URUICHI, Mikio; YAKUSHI, Kyuya; MOCHIDA, Tomoyuki[1]**
*([1]Toho Univ.)*

The ionic crystal $D^+A_3^-$ (D = dineopentylbiferrocene and A = $F_1$TCNQ) undergoes a first-order phase transition, in which second ionization occurs to form a doubly ionized state, $D^{2+}A_3^{2-}$.[1)] This monovalent-to-divalent phase transition gradually occurs in a wide temperature range from 160 K to 100 K. X-ray diffraction experiments showed that the Bragg spots consist of pairs of spots between 160 K and 100 K. One set is assigned to the unit cell of high-temperature phase and another is assigned to the low-temperature phase. On decreasing temperature, the intensities of the spots of high-temperature phase decreased and those of low-temperature phase increased. This observation is strong evidence for the phase separation in the temperature range of 160 K–100 K.

The Raman spectrum above 160 K also showed a big change below 100 K. When the laser is focused on the area of 2 μm diameter, the Raman spectrum shows position dependence: Only the monovalent peak (1446 $cm^{-1}$) is found in some area, while the divalent peak (1431 $cm^{-1}$) is found in other area, and both peaks are observed at the boundary of the two areas. The thickness of the boundary is estimated to be ~10–15 μm. In this boundary, the intensity ratio of the monovalent and divalent peaks changes gradually. The boundary area is so thick that may involve monovalent and divalent domains smaller than 2 μm. We mapped the 100 μm × 200 μm area at the phase-separation temperature. In this area, we observed only macroscopic domains, the size of which changes depending on the temperature.

The Raman spectrum and X-ray diffraction experiments described above showed that macroscopic domains of the monovalent and divalent phases coexist between 160 K and 100 K and the volume fraction of the two phases continuously changes in this phase-separation temperature region.

**Reference**

1) T. Mochida, K. Takazawa, M. Takahashi, M. Takeda, Y. Nishio, M. Sato, K. Kajita, H. Mori, M. M. Matsushita and T. Sugawara, *J. Phys. Soc. Jpn.* **74**, 2214 (2005).

# IV-B Magnetic Resonance Studies for Molecular-Based Conductors

Molecular based conductors are one of the extensively studied materials. The development of the understanding of the electronic phases of these materials enables us systematic investigations of low-dimensional highly correlated electrons systems. Competition of the electronic phases in molecular based conductors has attracted much attention. Magnetic resonance investigations are powerful investigations to understand the fundamental electronic properties, because they are microscopic and also dynamical measurements. The investigations of such electronic phases by means of magnetic resonance measurements are important to understand the unsolved fundamental problems in the field of solid state physics.

In this project, we performed the multi-frequency- (X-, Q- and W-bands) and pulsed-ESR, and broad-line NMR measurements for molecular based conductors to understand the electron spin dynamics in the low temperature electronic phases.

## IV-B-1 Charge Disproportionation in $(TMTTF)_2SCN$ Observed by $^{13}C$ NMR

**FUJIYAMA, Shigeki; NAKAMURA, Toshikazu**

[*Phys. Rev. B* **70**, 045102 (6 pages) (2004)]

The results of the $^{13}C$ NMR spectra and nuclear spin-lattice relaxation rate $1/T_1$ for the quasi-one-dimensional quarter-filled organic material $(TMTTF)_2SCN$ are presented. Below the anion ordering temperature ($T_{AO}$), a new broad line appears in the NMR spectra and the intensity of the distinct line owing to the inner carbon site from the inversion center is almost halved. The remarkable difference in the temperature dependence of $1/T_1$ below $T_{AO}$ for the two sharp lines corresponding to outer and inner carbon sites shows the development of a local electronic state. Our simple model of a charge configuration based on the electrostatic interaction between the SCN anions and TMTTF molecules is consistent with our observation of a local gap for the spin excitation. Nevertheless, we reveal that only the electrostatic interaction is insufficient to reproduce the observed divergence of the frequency shift and the linewidth of the newly appearing broad line stemming from the charge-accepting inner site at a much lower temperature than $T_{AO}$.

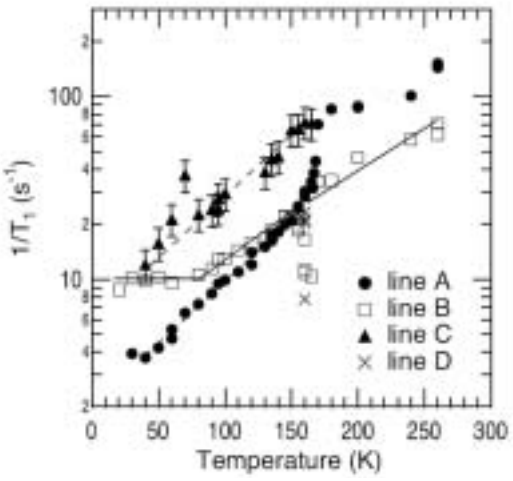


**Figure 1.** Nuclear spin-lattice relaxation rates for distinct lines. The solid and dashed lines are guides to the eye.

## IV-B-2 Redistribution of Electronic Charges in the Spin-Peierls State in $(TMTTF)_2AsF_6$ Observed by $^{13}C$ NMR

**FUJIYAMA, Shigeki; NAKAMURA, Toshikazu**

[*J. Phys. Soc. Jpn.* in press]

We report the results of $^{13}C$ NMR spectra and nuclear spin lattice relaxation rate $1/T_1$ for a quasi-one-dimensional quarter-filled organic material $(TMTTF)_2AsF_6$, which undergoes charge ordering ($T_{CO}$ = 102 K) and spin-Peierls phase transitions ($T_{SP}$ = 12 K). The ratio of two $1/T_1$ for the charge accepting and donating sites which grows from $T_{CO}$ finally saturates in approaching $T_{SP}$, that indicates an opening of single gap for the spin excitation spectra. At $T_{SP}$, however, doubly split NMR lines from inequivalently charged molecules merge originated from the variation in charge densities. This shows a rearrangement of the charge configuration in the spin-Peierls state.

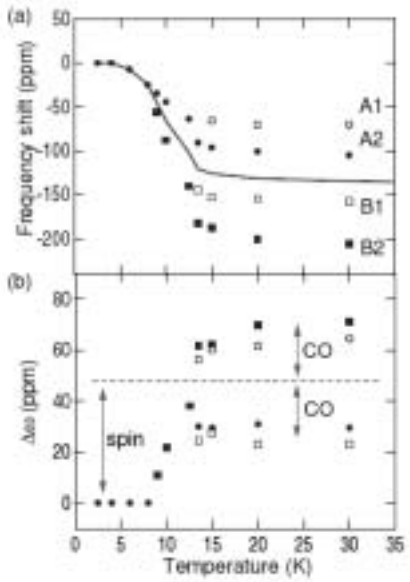


**Figure 1.** (a) The peak positions in the vicinity and below $T_{SP}$. (b) The gaps between the peak positions and the averaged frequency denoted as the solid line in (a). The dashed line shows the spin contribution to Δω.

### IV-B-3 Deuteration Effect and Possible Origin of the Charge-Ordering Transition of $(TMTTF)_2X$

**FURUKAWA, Ko; HARA, Toshifumi; NAKAMURA, Toshikazu**

[*J. Phys. Soc. Jpn.* in press]

ESR, NMR and X-ray measurements were performed for pristine and fully perdeuterio-TMTTF, TMTTF-$d_{12}$ salts. Significant enhancement by deuteration of the charge-order phase transition temperature, $T_{CO}$, was observed in ESR measurements for all $(TMTTF)_2X$ salts measured. No obvious relation between the $SbF_6$ anion motion and the TMTTF charge-order was found by $^{19}F$ NMR. We also performed single crystal X-ray measurements to understand the deuteration effects and temperature dependence of the crystal structure. A possible relationship between the $T_{CO}$'s and crystallographical parameters is proposed. The deuteration effects and possible origin of the charge-ordering transition of TMTTF salts are discussed.

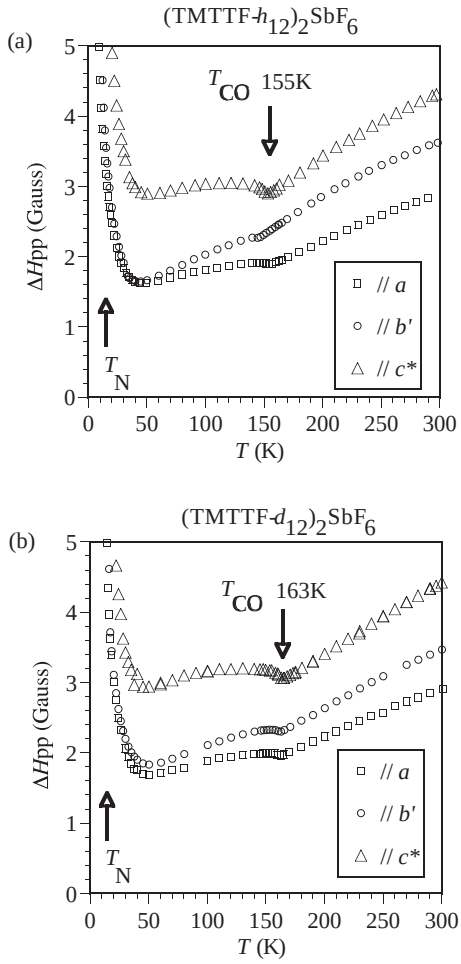


**Figure 1.** Temperature dependence of the ESR linewidth, $\Delta H_{pp}$, of (a) pristine, $(TMTTF\text{-}h_{12})_2SbF_6$ and (b) deuterated, $(TMTTF\text{-}d_{12})_2SbF_6$.

### IV-B-4 Redistribution of Electronic Charge in $(TMTTF)_2ReO_4$: $^{13}C$ NMR Investigation

**NAKAMURA, Toshikazu; HARA, Toshifumi; FURUKAWA, Ko**

[*J. Low Temp. Phys.* in press]

$^{13}C$ NMR measurements were performed for a one-dimensional organic conductor, $(TMTTF)_2ReO_4$. An intermediate charge-ordering (CO) phase has been found firstly for a TMTTF salt with a $T_d$-symmetry counter anion: The NMR parameters indicate two inequivalent molecules with unequal electron densities below 225 K. Moreover, the spin-singlet transition associated with $ReO_4$ anion ordering was confirmed at around 158 K by $^{13}C$ NMR measurements. A drastic change of NMR parameters below 158 K also indicates a redistribution of the electronic charge at the anion ordering temperature.

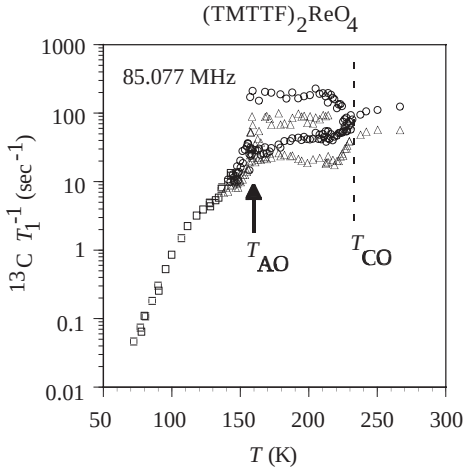


**Figure 1.** Temperature dependence of the $^{13}C$ NMR spin-lattice relaxation rate, $^{13}C$ $T_1^{-1}$, of $(TMTTF)_2ReO_4$.

### IV-B-5 Spin Structure of Organic Conductors $(TMTTF)_2X$

**FURUKAWA, Ko; HARA, Toshifumi; NAKAMURA, Toshikazu**

Organic conductors, $(TMTTF)_2X$ ($X$ = Br, $SbF_6$, and $PF_6$), are examined by electron spin resonance (ESR) spectroscopy, X-ray diffraction and theoretical calculation of $g$-tensor. In the case of the counter anions with octahedral symmetry, the anomalous change of the principal values and axes of the $g$-tensor, which were determined by the angular dependence of $g$-values, were observed in the temperature range from 20 K to the room temperature. However, the $g$-tensor was temperature independence in the Br salt. The temperature variation of the crystal structure for both salts is performed by X-ray diffraction. No obvious change of the molecular structure is observed in both salts. In the octahedral counter anion salts, the distance between the TMTTF molecules and the counter anion shrank due to the bulk counter anion as the temperature decreased. In order to interpret the anomalous $g$-shift, the theoretical calculation of the $g$-tensor based on the DFT-GIAO method is carried out. The relationship between the spin and the crystal structure will be discussed.

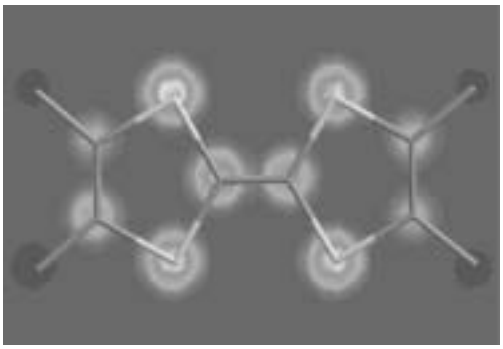

**Figure 1.** Spin density of the TMTTF radical determined by the DFT-GIAO method.

### IV-B-6 Multi-Frequency ESR Measurements for $(TMTTF)_2X$

**HARA, Toshifumi; FURUKAWA, Ko; NAKAMURA, Toshikazu**

TMTTF family salts are now attracted attention by the recent progress of the charge ordering (CO) investigations. Recently, we proposed the possible charge ordering configurations for each of $(TMTTF)_2X$ salts according to the difference of the ESR linewidth anisotropy at low temperatures. The CO configurations of $(TMTTF)_2X$ are roughly divided into three groups, and this classification is consistent with the results determined by other measurements. However the origin of the charge ordering phenomena is not clarified, and the quantitative understanding of the ESR linewidth is not succeeded so far. So we performed multi-frequency (X- [10GHz], Q- [30GHz], and W-bands [100GHz]) ESR measurements for one of typical TMTTF salts, $(TMTTF)_2SbF_6$, which shows the charge ordering transition at 154 K. The ESR linewidth determined by the W-band measurement is obviously larger than that by X-band below the charge ordering transition. We discuss the low temperature electron spin dynamics from the ESR point of view.

### IV-B-7 Extremely Slow Charge Fluctuations in the Metallic State of the Two-Dimensional Molecular Conductor θ-$(BEDT\text{-}TTF)_2RbZn(SCN)_4$

**CHIBA, Ryo[1]; HIRAKI, Ko-ichi[1]; TAKAHASHI, Toshihiro[1]; YAMAMOTO, M. Hiroshi[2]; NAKAMURA, Toshikazu**
*([1]Gakushuin Univ.; [2]RIKEN)*

[*Phys. Rev. Lett.* **93**, 216405 (4 pages) (2004)]

Large charge disproportionation has been confirmed in the metallic state of a 1/4-filled organic conductor θ-$(BEDT\text{-}TTF)_2RbZn(SCN)_4$ by means of $^{13}C$-NMR analysis on a selectively $^{13}C$-enriched single crystal sample. By comparing the homogeneous and inhomogeneous linewidths, the temperature dependence of the extremely slow dynamics of charge fluctuations has been determined first. The exotic nature of the metallic state of this salt is discussed.

### IV-B-8 Sliding Spin-Density Wave of $(TMTSF)_2PF_6$ Studied with Narrow-Band Noise

**SEKINE, Tomoyuki[1]; SATOH, Norikazu[1]; NAKAZAWA, Mitsuhiro[1]; NAKAMURA, Toshikazu**
*([1]Sophia Univ.)*

[*Phys. Rev. B* **70**, 214201 (13 pages) (2004)]

We report narrow-band noise (NBN) due to sliding motions of the spin-density wave (SDW) condensate at 2.0 K in three samples of $(TMTSF)_2PF_6$ and the magnetic-field effects. Typical NBN spectra coming from the saw-toothed-wave current oscillations are clearly observed. The periodic peaks due to the $4k_F$-charge-density wave (CDW) collective excitation are found, together with the SDW moving with a faster velocity, revealing that the sliding mode of the SDW is coupled with $4k_F$-CDW fluctuations. Observation of the interference peaks gives evidence of spatially non-uniform dc current carried by the deformable SDW in domains. At large currents the NBN spectrum drastically changes with increasing current and depends on applied magnetic field, suggesting a dynamical phase transition from the plastic-flow phase to the moving-solid phase. In the moving-solid phase the frequencies of the periodic peaks decrease with increasing current because the spatial coherency grows rapidly. The current oscillations in this phase are interpreted in terms of the coexistence of the $2k_F$-CDW collective excitation with the phason.

## IV-C Synchrotron X-Ray Diffraction Experiments and MEM Analyses for Single Crystals of Organic Conductors

By recent development of aggressive experimental and theoretical researches, electronic phases of organic conductors have been clarified so far. The remarkable anisotropy (low-dimensionality), small band-width and flexibility of the lattice are the characteristics of organic conductors. In most cases, band-structures of organic conductors are deduced with frontier orbitals (the highest occupied molecular orbital: HOMO as for a donor molecule, for example) estimated by molecule orbit calculations applying the tight-binding approximation. The Fermi surfaces calculated above correspond very well with that estimated from quantum vibration and/or angular dependence magneto-resistance experiments. Consistency with first principle calculations is also good. Theses facts

indicate that most of physics phenomena can be explained within the framework that the frontier orbital can be treated as if one rigid atomic orbital in an alkaline metal. The main aims of this project are, 1) to study whether there is a change of symmetry of frontier orbitals (electric charge distribution in molecules), which is believed to be rigid so far, at phase transitions, and 2) to investigate possible relation between the detailed electric charge distribution in molecules and the electronic phases. Of course, the tight-binding approximation with a rigid frontier orbital is firm to be very good approximation. However, there are several experimental results which suggest a change of electric charge distribution in the molecule in some systems. We performed synchrotron X-ray diffraction experiments and MEM (The Maximum Entropy Method) analyses to investigate the electric charge distribution of molecules for such interesting systems.

This project is partially supported by Grant-in-Aid for Creative Scientific Research Collaboratory on Electron Correlation-Toward a New Research Network between Physics and Chemistry- (13NP0201) from the Ministry of Education, Culture, Sports, Science and Technology, Japan.

### IV-C-1 Low-Temperature Charge-Ordering State of $(TMTTF)_2PF_6$

**HARA, Toshifumi; FURUKAWA, Ko; KAKIUCHI, Toru[1]; SAWA, Hiroshi[2]; NAKAMURA, Toshikazu**
*([1]SOKENDAI; [2]KEK)*

As for the charge-ordering problem which is one of the recent hot topics, electronic charge configurations at low temperatures are clarified so far by several groups containing us. The importance of the long-range Coulomb interaction is pointed out by theoretical researches. TMTTF family salts have been attracting attention due to observations of their charge-ordering (CO) phenomena. $^{13}C$ NMR indicates the existence of inequivalent TMTTF sites at low temperatures, and dielectric permittivity measurements show ferroelectric behaviors for $(TMTTF)_2MF_6$ ($M$ = P, As, Sb) salts. We also proposed that the variation of charge-ordering patterns such as –O–O–o–o– and –O–o–O–o– along the stacking axes for a series of TMTTF salts by ESR linewidth analyses. However, as for the research of the charge-ordering, the electric charge distribution in the molecule was ignored so far. Hence we performed synchrotron X-ray diffraction measurements and MEM analyses to investigate the electric charge distribution of molecules and to understand the low-temperature charge-ordering state of $(TMTTF)_2PF_6$. Figure shows the charge distribution of $(TMTTF)_2PF_6$ at R.T. Further investigations are now underway.

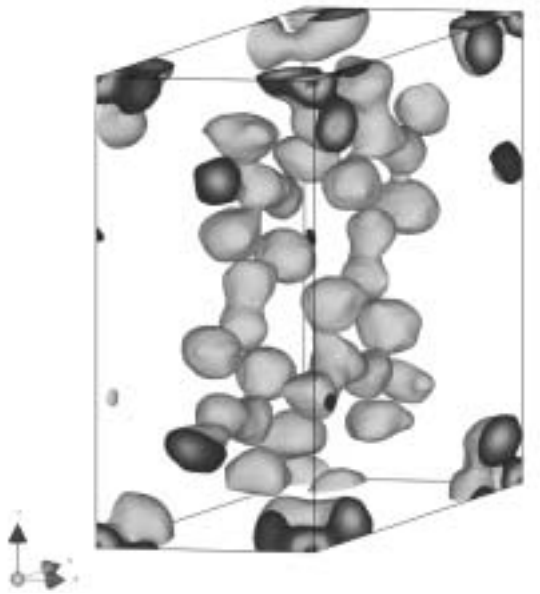

**Figure 1.** Charge distribution of $(TMTTF)_2PF_6$ at R.T. determined by synchrotron X-ray diffraction measurements and MEM analyses.

## IV-D EPR Study toward Molecular Biology as Microscopic and Selective Probes Measurements

The structure analyses of the material related to fundamental biology are now hot topics. Especially synchrotron X-ray measurements attract much attention since they can provide detail of the structural information. However, X-ray measurements can be applied only for crystalline material, the resolution is not so good. On the other hand, EPR measurements are advantageous because they are microscopic and selective probes and they can provide dynamical information. Hence, we performed the multi-frequency- and pulsed-ESR for such kind of materials to understand the local structure and possible mechanism of several biological processes.

## IV-D-1 First Detection of the Multiline Signal from the $S_2$-State Manganese Cluster of Photosystem II by Single-Crystal W-Band EPR Spectroscopy

**MATSUOKA, Hideto[1]; SHEN, Jian-Ren[2]; MINO, Hiroyuki[3]; FURUKAWA, Ko; KATO, Tatsuhisa[4]; KAWAMORI, Asako[5]**

*([1]IMS and Free Univ. Berlin; [2]Okayama Univ.; [3]Nagoya Univ.; [4]IMS and Josai Univ.; [5]Kwansei Gakuin Univ. )*

[*J. Phys. Chem. B* submitted]

The multiline signal from the $S_2$-state manganese cluster in the oxygen evolving complex of photosystem II (PSII) was observed in single crystals of a thermophilic cyanobacterium *Thermosynechococcus vulcanus* for the first time by W-band (95 GHz) electron paramagnetic resonance (EPR), as shown in the figure. The single-crystal spectra were reasonably interpreted by spectral simulation with the hfc parameters appropriate for a trimer-monomer structure of the cluster. The use of PSII single crystals allowed us to determine precisely the *g*-tensor of the cluster. The principal values of the tensor indicated that the Mn(III) ion in the cluster exists in an approximate axial symmetry. This work demonstrated that single-crystal experiments are crucial to detect the distinct resolved hfs of the $S_2$ state at W-band.

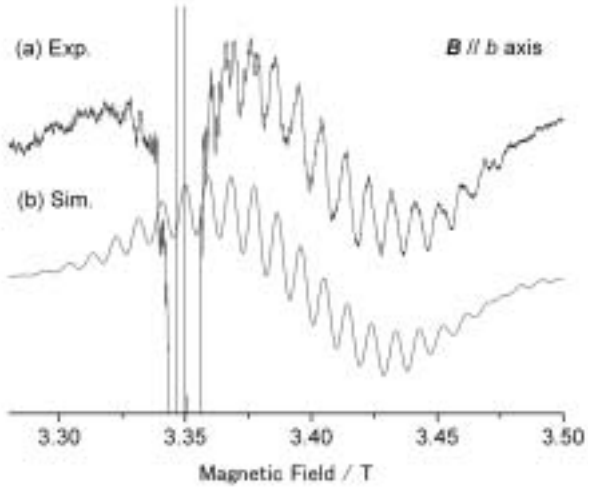


**Figure 1.** (a) Light-minus-dark W-band EPR spectra observed at 6 K for the $S_2$ state in single crystals of PSII form *T. vulcanus*. (b) The best-fit simulation of (a). The crystallographic *b*-axis was approximately parallel to the direction of the magnetic field.

# IV-E Development of Multi-Functional Molecular Systems

Since the molecules tend to retain their independence even in the solid state, the molecular systems can be considered to be suitable systems to construct multi-functional systems by assembling various molecular building blocks with different characters. We are trying to develop various new functional molecular materials such as single-component molecular conductors, photo-controllable magnetic conductors and dielectrically active porous molecular systems.

Recently, "dual-action organic conductors" such as magnetic molecular conductors have attracted a considerable interest. We have discovered unprecedented conductors exhibiting "superconductor → insulator transition," (λ-$(BETS)_2Fe_xGa_{1-x}Cl_4$, BETS = bis(ethylendithio)tetraselenafulvalene) and the antiferromagnetic organic superconductors (κ-$(BETS)_2FeX_4$ X = Br, Cl) and the field-induced organic superconductor (λ-$(BETS)_2FeCl_4$, λ-$(BETS)_2Fe_xGa_{1-x}Cl_4$, κ-$(BETS)_2FeBr_4$). However, except these systems, there have been only a few systems showing clear synergetic actions between conduction and magnetic parts. Very recently, we have discovered "constant resistivity state (CRS)" below $T_c$ in the system exhibiting superconductor → insulator transition at zero magnetic field (λ-$(BETS)_2Fe_xGa_{1-x}Cl_4$, $x \approx 0.35$).

We have recently obtained a new κ-type BETS conductor with weakly ferromagnetic (canted antiferromagnetic) metal state and new molecular conductors exhibiting spin-crossover transition coupled with resistivity hysteresis and LIESST (Light-Induced Excited Spin State Trapping).

By utilizing weak host-guest interaction and polarizability of guest molecules, we have recently obtained new porous molecular systems with high-temperature polarizable and low-temperature unpolarizable states.

Besides these systems, we have recently developed the single-component molecular metals based on the transition metal with extended-TTF ligands. $Au(tmdt)_2$, which is isostructural to the first single-component molecular metal $Ni(tmdt)_2$ is the first molecular conductor where π conduction electron and antiferromagnetic order coexist above 100 K.

## IV-E-1 Dielectric Properties of Porous Molecular Crystals Containing Polar Molecules

**CUI, HengBo; TAKAHASHI, Kazuyuki; OKANO, Yoshinori; KOBAYASHI, Hayao; WANG, Zheming[1]; KOBAYASHI, Akiko[2]**
*([1]Peiking Univ.; [2]Univ. Tokyo)*

[*Angew. Chem., Int. Ed.* **117**, 6666–6670 (2005)]

Recently molecular materials with porous coordination frameworks have aroused a considerable interest because of their various attractive properties arising from the synergy of the host lattice and guest molecules such as guest-switched spin crossover transition, gas sorption, molecular storage, and magnetic solvent sensor. However, to our knowledge, the reports on the dielectric properties of porous molecular materials seem to be very rare, though ferroelectric properties of molecular materials have recently attracted an increasing interest. We have recently obtained molecular systems exhibiting unprecedented dielectric properties by combining a porous ferrimagnetic molecular crystal, $[Mn(HCOO)_2]$ and polar guest molecules, $H_2O$ and $CH_3OH$. $[Mn_3(HCOO)_6](H_2O)(CH_3OH)$ showed characteristic temperature-dependent dielectric constant for *E*//*a*, *b* but featureless behavior for *E*//*c*. It is very interesting that molecules confined in the narrow one-dimensional channel show a fairly sharp "transition-*like* behavior" because in general the system with strong one-dimensional nature hardly exhibits the phase transition.

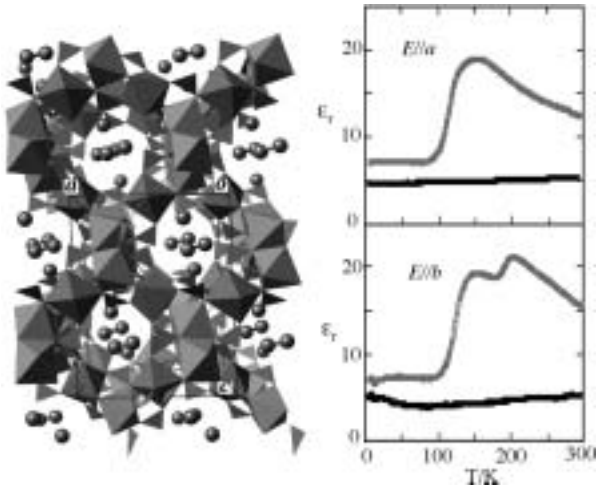


**Figure 1.** Crystal structure and dielectric constants of $[Mn_3(HCOO)_6](H_2O)(CH_3OH)$. The spheres in the channel are C and O atoms of the guest molecules. The black lines are the dielectric constants of the crystal without guest molecules.

## IV-E-2 Giant Dielectric Constants of Porous Molecular Crystal with Guest Water Cluster

**CUI, HengBo; LONG, La-Sheng; TAKAHASHI, Kazuyuki; OKANO, Yoshinori; KOBAYASHI, Hayao; KOBAYASHI, J. Akiko[1]; KOBAYASHI, Akiko[1]**
*([1]Univ. Tokyo )*

Except for the ferroelectric (or anti-ferroelectric) materials, the heavy metal compounds such as $PbCl_2$ ($\varepsilon_r$ = 33.5 (20 °C)), PbO ($\varepsilon_r$ = 25.9 (20 °C)), and TlBr ($\varepsilon_r$ = 30.3 (25 °C)) are known to be typical materials with large dielectric constants. It will be desirable to find a way to develop such highly polarizable materials with-

out pernicious heavy metal atoms, especially molecular materials with dielectric properties switchable between high and low dielectric states. Since most molecules have no positional freedom in the crystalline state, the dielectric constants of molecular crystals are usually very small and almost temperature independent. On the other hand, there exist polar molecules with fairly large polarizabilities in the liquid state. Needless to say, the water is the exceptional system with very large dielectric constant, which becomes as high as 100 just above the freezing point (supercooled state). This value is about 40 times lager than that of benzene. We have examined the dielectric properties of water cluster formed in the channel of porous molecular crystal, $Cu_3La_2(NH(CH_2COO)_2)_6$ and found the extremely large enhancement of the dielectric constants around room temperature. To our surprise, the dielectric constant seems to exceed 200 at high temperature.

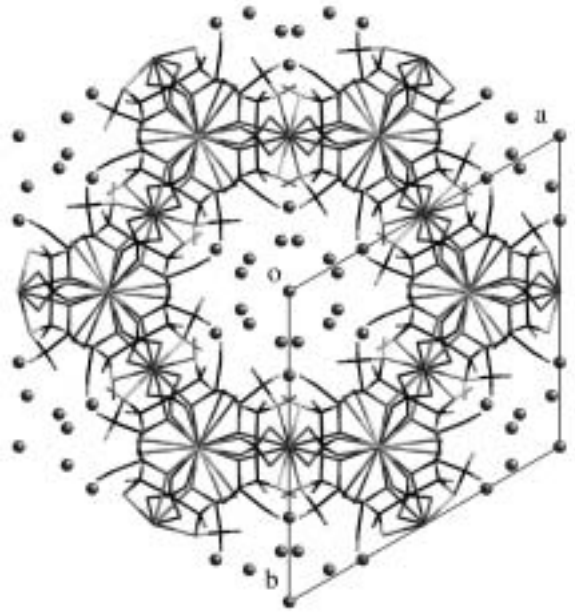


**Figure 1.** Crystal structure of $Cu_3La_2(NH(CH_2COO)_2)_6$ viewed along the *c* axis of the hexagonal porous crystal. The spheres in the channel are O atoms of water molecules forming one-dimensional water cluster.

### IV-E-3 Synthesis and Characterization of a Porous Magnetic Diamond Framework Compound, $Co_3(HCOO)_6$, and Its $N_2$ Sorption Characteristic

**WANG, Zheming[1]; ZHANG, Bin[2]; KURMOO, Mohamedally[3]; GREEN, Mark, A.[4]; OTSUKA, Takeo; KOBAYASHI, Hayao**
*([1]Peiking Univ.; [2]IC, CAS; [3]Univ. Louis Pasteur; [4]Royal Inst.)*

[*Inorg. Chem.* **44**, 1230–1237 (2005)]

$[Co_3(HCOO)_6](CH_3OH)(H_2O)$, the iso-structural analogue of the porous magnet of coordination framework $[Mn_3(HCOO)_6](CH_3OH)(H_2O)$, was prepared by slow diffusion technique and characterized by X-ray and neutron diffraction methods, IR, TGA-DSC and BET and its magnetic properties measured. It crystallizes in the monoclinic system, space group $P2_1/c$, $a$ =11.247(2), $b$ = 9.812(2), $c$ = 18.103(3) Å, β = 127.245(3)°, $V$ = 1590.3(5) Å$^3$, $Z$ = 4, $R_1$ = 0.0356 (determined from single crystal data at 87 K) and it possesses a unit cell volume that is 10% smaller than $[Mn_3(HCOO)_6](CH_3OH)(H_2O)$ due to the smaller radius of $Co^{2+}$ ion. The cell parameters, obtained from neutron powder data at 2 K, are $a$ = 11.309(2), $b$ = 9.869(1), $c$ = 18.201(3) Å, β = 127.244(8)°, $V$ = 1617.3(5) Å$^3$. The pore volume also reduces from 33% to 29% by replacing Mn by Co. The material exhibits an interesting diamond framework based on Co-centered $CoCo_4$ tetrahedral nodes, in which all metal ions have octahedral coordination geometry and all HCOO groups link the metal ions in *syn-syn*/*anti* modes. It displays high thermal stability up to 270 °C. The compound easily loses the guest molecules without loss of crystallinity and it partly re-absorbs water from the atmosphere. Significant $N_2$ sorption was observed for the desolvated framework suggesting the material possesses permanent porosity. The magnetic properties show a tendency to a 3D long-range magnetic ordering, probably antiferromagnetic with a spin canting arrangement below 2 K.

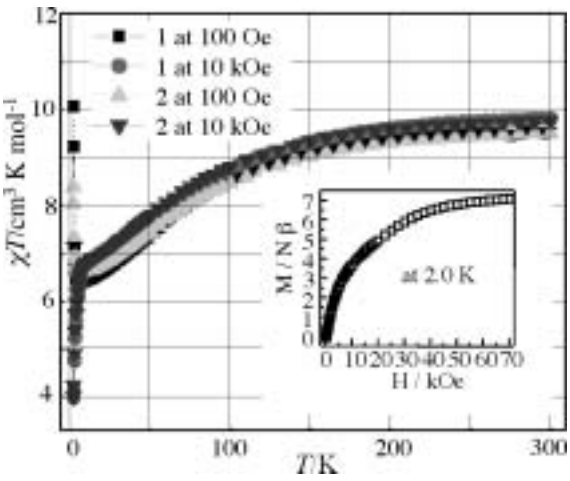


**Figure 1.** The temperature dependence of the magnetic susceptibility of **1** ($[Co_3(HCOO)_6](CH_3OH)(H_2O)$) and desolvated form **2** ($[Co_3(HCOO)_6]$) in applied field of 100 Oe and 10 kOe. Inset is the isothermal field dependent magnetization at 2.0 K for **1**. Magnetization at 70 kOe is 7.10 Nβ.

### IV-E-4 Superconductivity and Voltex Phases in the Two-Dimensional Organic Conductor λ-$(BETS)_2Fe_xGa_{1-x}Cl_4$ ($x$ = 0.45)

**UJI, Shinya[1]; TERASHIMA, Taichi[1]; YASUZUKA, Shuma[1]; TOKUMOTO, Madoka[2]; TANAKA, Hisashi[2]; KOBAYASHI, Akiko[3]; KOBAYASHI, Hayao**
*([1]Natl. Inst. Mater. Sci.; [2]AIST; [3]Univ. Tokyo)*

[*Phys. Rev. B* **71**, 104525 (7 pages) (2005)]

Resistance measurements have been performed in two-dimensional organic conductor λ-$(BETS)_2Fe_xGa_{1-x}Cl_4$ ($x$ = 0.45) to investigate the superconducting proper-

ties. In magnetic field parallel to the layers, the superconducting (S) phase is stabilized in a wide mag netic field range, which is qualitatively understood by Jaccarino-Peter compensation mechanism. Depending on the internal field produced by the Fe 3d moments, three vortex phases in the S phase appear with increasing field. The superconducting transitions show characteristic field dependence, which is correlated to the voltex phases. In field perpendicular to the layers, the S phase appear only near the antiferromagnetic phase. The results for $x = 0.45$ are also compared with those for the isostructural nonmagnetic salt $x = 0$.

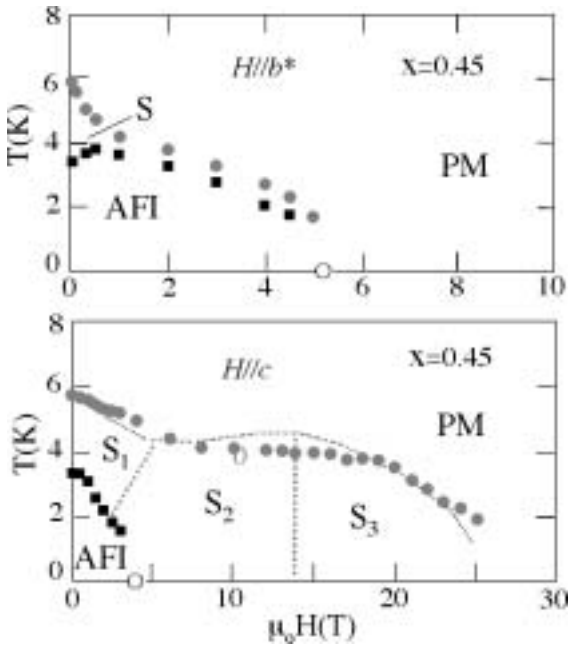


**Figure 1.** *T-H* phase diagram of λ-$(BETS)_2Fe_xGa_{1-x}Cl_4$ ($x$ = 0.45) for *H*//*b** and *H*//*c*.

## IV-E-5 Constant Resistivity State in the Field-Induced Organic Superconductor, λ-$(BETS)_2Fe_xGa_{1-x}Cl_4$

**CUI, HengBo; TAKAHASHI, Kazuyuki; KOBAYASHI, Hayao; KOBAYASHI, Akiko[1]**
*([1]Univ. Tokyo)*

In 2001, Uji *et al.* have discovered the field-induced superconductivity (FISC) in two-demensional organic conductor, λ-$(BETS)_2FeCl_4$ with π-d coupled antiferromagnetic insulationg ground state below 8.5 K. Balicas *et al.* have found the FISC to be most stabilized around 33 T. Similar FISC states were also observed in a series of mixed-anion systems, λ-$(BETS)_2Fe_xGa_{1-x}Cl_4$. We have also reported the unprecedented resistivity switching between insulating, superconducting and metallic states in λ-$(BETS)_2Fe_xGa_{1-x}Cl_4$ ($x \approx 0.4$). We have recently reexamined the resistivity of λ-$(BETS)_2Fe_xGa_{1-x}Cl_4$ ($x \approx 0.4$) up to 15 T at the temperature range down to 1 K. The crystal with $x = 0.37$ exhibited a superconducting transition at 4.6 K and superconductor-insulator transition around 2.3 K at zero magnetic field. But the superconducting state was changed to "the temperature- and field-independent resistivity state" with increasing magnetic field applied parallel to *ac* conduction plane. This constant resistivity state (CRS) was also observed in the crystals with $x \approx 0.39$, 0.37 (other crystal) and 0.30. But three crystals with $x$-value higher than 0.43 did not show CRS. The ratio of the resistivity of CRS ($\rho_c$) and the resistivity just above the superconducting transition ($\rho_m$), that is, $\rho_m/\rho_c$ is linearly dependent on $x$. To our knowledge, λ-$(BETS)_2Fe_xGa_{1-x}Cl_4$ ($x \approx 0.35$) is the first superconductor showing CRS.

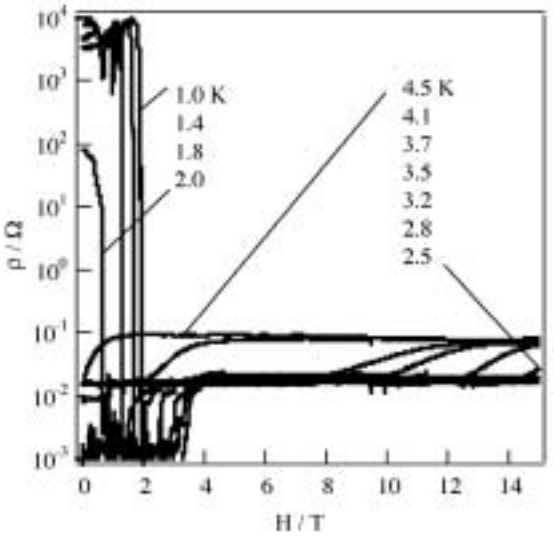


**Figure 1.** Low-temperature resistivity behavior of λ-$(BETS)_2Fe_xGa_{1-x}Cl_4$ ($x$ = 0.37) under the magnetic field applied parallel to the *ac* conduction plane.

## IV-E-6 (Tetrathiafulvalene)[$Fe^{III}(C_2O_4)Cl_2$]: An Organic-Inorganic Hybrid Exhibiting Canted Antiferromagnetism

**ZHANG, Bin[1]; WANG, Zheming[2]; FUJIWARA, Hideki; KOBAYASHI, Hayao; KURMOO, Mohamedally[3]; INOUE, Katsuya[4]; MORI, Takehiko[5]; GAO, Song[2]; ZHANG, Yan[2]; ZHU, Daoben[1]**
*([1]IC CAS; [2]Peiking Univ.; [3]Univ. Louis Pasteur; [4]Hiroshima Univ.; [5]TIT)*

[*Adv. Mater.* **17**, 1988–1991 (2005)]

Over the past twenty years, the field of molecular materials has been decorated with a wide range of interesting compounds, based either on purely organic or inorganic molecules and organic-inorganic hybrids, exhibiting diverse electrical, magnetic and optical properties. While several electrical and magnetic ground states have been established and very well documented in the literature, the possibility of introducing novel properties with organic-inorganic hybrids remains a big challenge to date. The key feature of these hybrids is the interaction through space or through weak supramolecular contacts. While this can be quite strong between nearest neighbours having strong π-π overlap, especially those containing chalcogenides, the interactions between π-d are usually quite weak. To enhance the d-d super-exchange within the inorganic moiety, the use of 2D-polymeric anions containing oxalato bridges

has been very successful to produce magnetic systems. On the other hand, it appears that chalogen-halogen contacts may be a good source for the π-d coupling in compounds containing isolated $MX_4$ anions. The present work is an attempt to mixed oxalate and halogen at the metal site of the anions to introduce d-d superexchange and π-d interaction in charge-transfer complex. Recently, two coordination compounds with $C_2O_4^{2-}$ and $Cl^-$ have been reported and show ferromagnetic transition at 40 K and 70 K. We, therefore, present the first example of a TTF complex from a novel polymeric one-dimensional counter anion of iron that contains terminal chlorine and oxalate bridges. A new molecular-hybrid (TTF)[$Fe^{III}(C_2O_4)Cl_2$] displaying canted antiferromagnetism has been prepared and characterized. It is the first salt of TTF or its derivatives to contain a one-dimensional magnetic coordination polymer as anion. Due to π-d interaction, through short S···Cl, S···O contacts, a 3D-Néel state is stabilized at a rather high temperature of 20 K. It is a semiconductor with band gap of 1 eV.

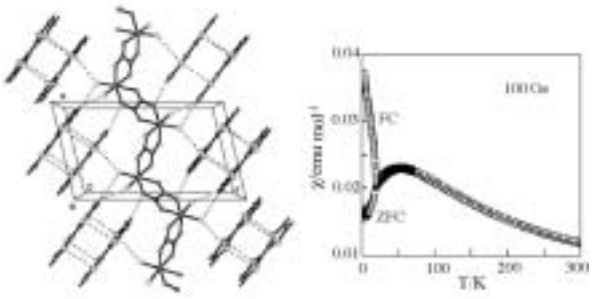


**Figure 1.** Crystal structure and zero-field cooling (ZFC) and field cooling (FC) M/H versus temperature curves of [TTF][Fe$(C_2O_4)Cl_2$].

### IV-E-7 Development of Single-Component Molecular Metals

**KOBAYASHI, Akiko[1]; ZHOU, Biao[1]; KOBAYASHI, Hayao**
*([1]Univ. Tokyo)*

[*J. Mater. Chem.* **15**, 3449–3451 (2005)]

Our recent studies on single-component molecular metals was introduced. The realization of molecular metal based on single-component molecules had been one of the long-standing challenges in the chemistry of molecular conductors since the discovery of semiconducting properties of molecular crystals around 1950. In contrast to typical inorganic metals composed of single elements, such as Na and Au, all of the molecular metals developed until 2000 are composed of more than two chemical species. However, we have proved that the metal electrons can be generated automatically by the self-assembling of the same kind of molecules. The novel nickel complex with the extended-TTF dithiolate ligand [Ni(tmdt)$_2$] (tmdt = trimethylenetetrathiafulvalenedithiolate) is the first three-dimensional single-component molecular metal with metallic state down to 0.6 K. The isostructural molecular conductor [Au(tmdt)$_2$] exhibited an antiferromagnetic transition around 110 K without loss of its high conductivity, which is extraordinarily high compared with the magnetic transition temperatures of the other molecular conductors ever developed. A brief description was also presented on "single-component alloy system" [$Ni_xAu_{1-x}$(tmdt)$_2$].

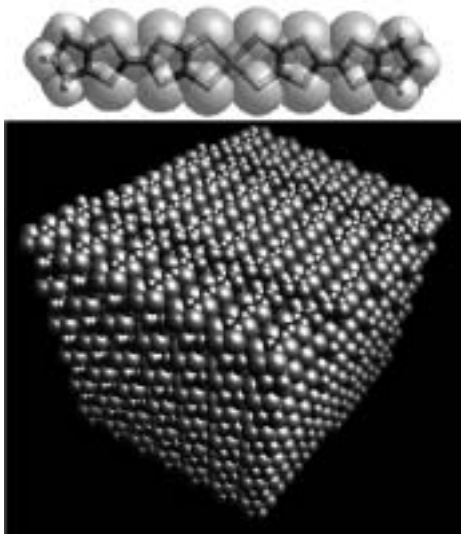

**Figure 1.** The molecular packing in single-component molecular metal [Au(tmdt)$_2$] which is the first molecular system exhibiting the coexistence of π conduction electrons and magnetic order above 100 K.

### IV-E-8 Crystal Structures and Physical Properties of Single-Component Molecular Conductors Consisting of Nickel and Gold Complexes with Bis(trifluoromethyl)-tetrathiafulvalenedithiolate Ligands

**SASA, Masaaki[1]; FUJIWARA, Emiko[1]; KOBAYASHI, Akiko[1]; ISHIBASHI, Shoji[2]; TERAKURA, Kiyoyuki[4]; OKANO, Yoshinori; FUJIWARA, Hideki; KOBAYASHI, Hayao**
*([1]Univ Tokyo; [2]AIST; [3]Hokkaiudo Univ.)*

[*J. Mater. Chem.* **15**, 155–163 (2005)]

The neutral nickel and gold complexes with bis-(trifluoromethyl)tetrathiafulvalenedithiolate ligands, [M(hfdt)$_2$] (M = Ni, Au) were prepared in order to examine the possibility of the development of single-component molecular conductors soluble to organic solvents. However, in contrast to the previous report, the crystals did not show any solubility to usual organic solvents. On the other hand, the crystal structure analysis showed unique two-dimensional layered structures, despite that the single-component molecular conductors usually tend to take compact three-dimensional molecular arrangement. Each layer is separated by the terminal $CF_3$ groups to form the "$CF_3$ bi-layer structure." The shortest intermolecular F···F distance (3.018 Å for [Ni(hfdt)$_2$] and 2.862 Å for [Au(hfdt)$_2$]) is significantly longer than the van der Waals F···F distance (2.70 Å) and the distribution of the frontier electrons is almost zero around the $CF_3$ bi-layer region. This is due to the strong F···F segregation effect, which will provide a

useful way to control the molecular aggregation in the single-component molecular conductors. The extended-Hückel tight-binding band structure calculations and the *ab-initio* local density approximation (LDA) band structure calculations were made for $[Ni(hfdt)_2]$, which can explain the semiconducting and non-magnetic properties of the system. The extended-Hückel tight-binding band structure calculations were also made for $[Au(hfdt)_2]$. The calculated band structure is consistent with weakly semiconducting and almost non-magnetic properties of $[Au(hfdt)_2]$.

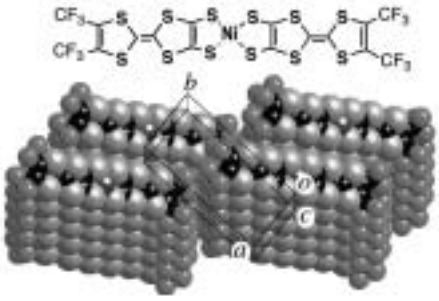


**Figure 1.** The molecular packing of $[Ni(hfdt)_2]$.

### IV-E-9 *Ab Initio* Electronic Structure Calculation of Single-Component Molecular Conductor $Au(tmdt)_2$ (Tmdt = Trimethylene-tetrathiafulvalenedithiolate)

**ISHIBASHI, Shoji[1]; TANAKA, Hisashi[1]; TOKUMOTO, Madoka[1]; KOBAYASHI, Akiko[2]; KOBAYASHI, Hayao; TERAKURA, Kiyoyuki[3]**
*([1]AIST.; [2]Univ. Tokyo; [3]Hokkaido Univ.)*

[*J. Phys. Soc. Jpn.* **74**, 843–846 (2005)]

We have investigated the electronic structure of $Au(tmdt)_2$ (tmdt = trimethylenetetrathiafulvalene-dithiolate), which is a single-component conductor showing a magnetic phase transition around 100 K, by *ab initio* plane-wave pseudopotential calculations. A single band crosses the Fermi level. This band and the next band below are a result of the strongly hybridization between the two neighbouring molecular levels near the Fermi level (SOMO and HOMO-1) and the system is more properly described as quater-filled rather than half-filled in the strong correlation regime. The Fermi surface has corrugated-sheet-like parts nearly parallel to each other. Interband generalized susceptibility suggests the presence of a nesting vector $a^*/2$. Spin-polarized calculation on the doubled unit cell along the *a* axis results in an antiferromagnetic order. The nesting is not perfect and Fermi-surface pockets remain in the magnetic phase. The implications of the present calculations with regard to experimental results are discussed.

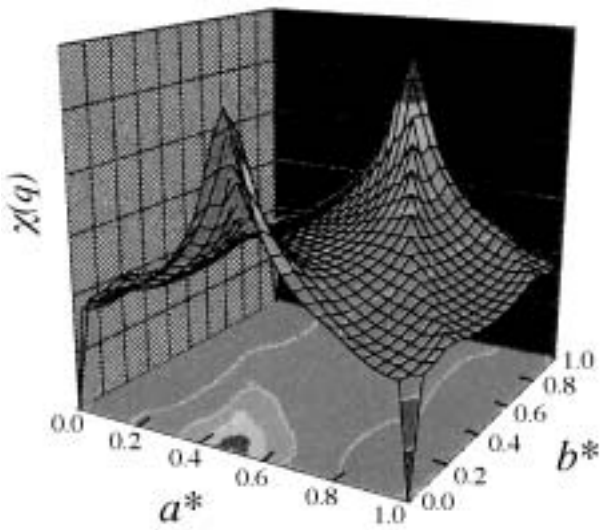


**Figure 1.** The interband generalized susceptibility of $[Au(tmdt)_2]$.

### IV-E-10 The Light-Induced Excited Spin State Trapping Effect on $Ni(dmit)_2$ Salt with an Fe(III) Spin-Crossover Cation: $[Fe(qsal)_2][Ni(dmit)_2]\cdot 2CH_3CN$

**TAKAHASHI, Kazuyuki; CUI, HengBo; KOBAYASHI, Hayao; EINAGA, Yasuaki[1]; SATO, Osamu[2]**
*([1]Keio Univ.; [2]Kyushu Univ.)*

[*Chem. Lett.* **34**, 1240–1241 (2005)]

Recently spin-crossover (SC) complexes have aroused a considerable attention in molecular materials scientists. Since the spin conversion between the low-spin (LS) and high-spin (HS) states can be induced by external perturbations such as temperature, pressure, and light, the introduction of the SC component is expected to give a switching ability to a molecular solid. The number of the reports of the LIESST effect on Fe(III) complexes is very rare. Therefore, realization of the LIESST in an Fe(III) SC component may be the first step to develop various photo-switchable molecular materials. We have focused our attention on the Fe(III) spin crossover complex, $[Fe(qsal)_2][Ni(dmit)_2]\cdot 2CH_3CN$ [qsalH = *N*-(8-quinolyl)-salicylaldimine, dmit = 4,5-dithiolato-1,3-dithiole-2-thione]. Temperature dependence of $\chi_M T$ in $[Fe(qsal)_2][Ni(dmit)_2]\cdot 2CH_3CN$ showed a cooperative spin transition (Figure 1a). On illumination with a diode laser (830 nm) at 5 K (Figure 1b), the magnetization of the complex gradually increased, indicating that the light-induced metastable HS state could be trapped. On heating after saturation of magnetization with light illumination, the relaxation from the metastable HS to the ground LS states was observed at around 40 K ($T_{LIESST}$ = 46 K). The magnetization curve of the annealing sample followed that before illumination. This indicates that the change by light is completely reversible. Furthermore, the decease in magnetization by illuminating the metastble HS state with a diode laser (980 nm) suggests that the magnetism of the 1:1 complex can be controlled by light irradiation.

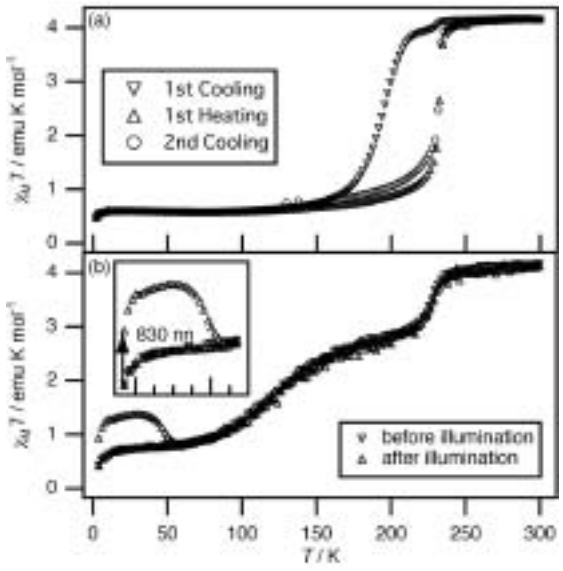


**Figure 1.** $\chi_M T$ *vs. T* plot of $[Fe(qsal)_2][Ni(dmit)_2]\cdot 2CH_3CN$: (a) Bulk sample, (b) the LIESST experiment of ground sample with an adhesive tape by using a diode laser (830 nm).

## IV-E-11 Synergic Behavior between Spin and Conducting Property in Ni(dmit)$_2$ Salt with Fe(III) Spin-Crossover Cation

**TAKAHASHI, Kazuyuki; CUI, HengBo; OKANO, Yoshinori; KOBAYASHI, Hayao; EINAGA, Yasuaki[1]; SATO, Osamu[2]**
*([1]Keio Univ.; [2]Kyushu Univ.)*

Recently considerable interest has been attracted to the development of novel molecular-based conducting materials exhibiting the synergy between conductivity and magnetism. We have attempted to explore the possibility of "dynamic" and "reversible" control of electrical conducting state by external stimuli. It is well known that the conducting properties of molecular conductors are changed greatly by the small modification of their crystal structures. Since the spin transition between the low-spin (LS) and the high-spin (HS) states accompanies a remarkable structural change in coordination bond length and geometry, the electrical conductivity of conducting spin-crossover (SC) complex can be expected to be "dynamically" and "reversibly" controlled by a structural change involving the spin conversion. The conducting complex was prepared by electrocrystallization of $[Fe(qsal)_2][Ni(dmit)_2]\cdot 2CH_3CN$ in acetonitrile. The crystal structure analyses revealed that the ratio of $Fe(qsal)_2$ and $Ni(dmit)_2$ proved to be 1 to 3. $Ni(dmit)_2$ anions formed one-dimensional columns along the *b* axis and were arranged in a herringbone manner along the side-by-side direction. Temperature dependence of magnetic moment and electrical resistivity of the 1:3 complex were shown in Figure 1. As a result of the cooling and heating processes, the magnetic behavior showed a narrow hysteresis loop with width of 8 K between 90 and 120 K. The change in $\chi_M T$ value, which was larger than that estimated for the antiferromagnetic coupling of spins of $Ni(dmit)_2$, seemed to derive from the spin transition. The crystal showed a semiconducting behavior ($\sigma_{RT}$ = 0.1 S cm$^{-1}$; $E_a$ = 0.2 eV). Interestingly, a hysteresis loop of resistivity was observed in the temperature range of 90–120 K, which corresponds to the temperature range of the hysteresis of magnetic behavior. The relatively low resistivity in heating process is consistent with the compact molecular packing usually observed in the LS state. To our knowledge, this is the first observation of the resistivity anormaly coupled with spin transition.

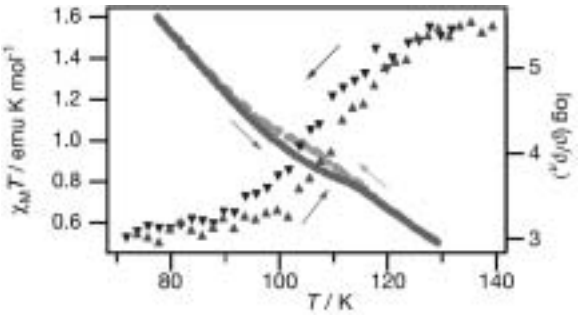


**Figure 1.** $\chi_M T$ *vs. T* plot (triangle, scale: left) and $\log(\rho/\rho_{rt})$ *vs. T* plot (circle, scale: right) of the 1:3 complex at the temperature range between 70 and 140 K.

## IV-E-12 Synthesis and Molecular Structure of a Novel PROXYL-Fused π-Electron Donor, PROXYL-ET-STF

**TAKAHASHI, Kazuyuki; KOBAYASHI, Hayao**

The development of novel magneto-electronic properties based on the interplay between conducting electrons and localized spins has aroused a great attention in molecular materials. To realize the coupling between conducting π-electrons and the spins on the stable organic radical in purely organic systems is one of the targets in this field. Despite several reports of syntheses and physical properties of π-electron donor or acceptor molecules with stable organic radicals and their conducting complexes, the number of metallic complexes based on these donors is rare. Probably since the organic stable radicals are usually bulky, it is difficult to construct the conduction path based on the overlap of π-donor parts. In order to decrease a hindrance to the formation of conduction path, we have designed and synthesized PROXYL-fused π-electron donor, PROXYL-ET-STF.

Synthesis of PROXYL-ET-STF is summarized in Scheme 1. The donor was isolated as fine needles and stable in air. X-ray structural analysis was performed on a single crystal of the neutral donor molecule. The molecular structure of PROXYL-ET-STF was a little bent, but the radical part was almost parallel to the 1,3-diselenol ring. Donor molecules were stacked in a head-to-tail manner to form one-dimensional columns. These observations suggest that PROXYL-ET-STF is a promising donor to afford conducting complexes with a stable organic radical. Physicochemical properties and preparation of the conducting complexes of this donor are now in progress.

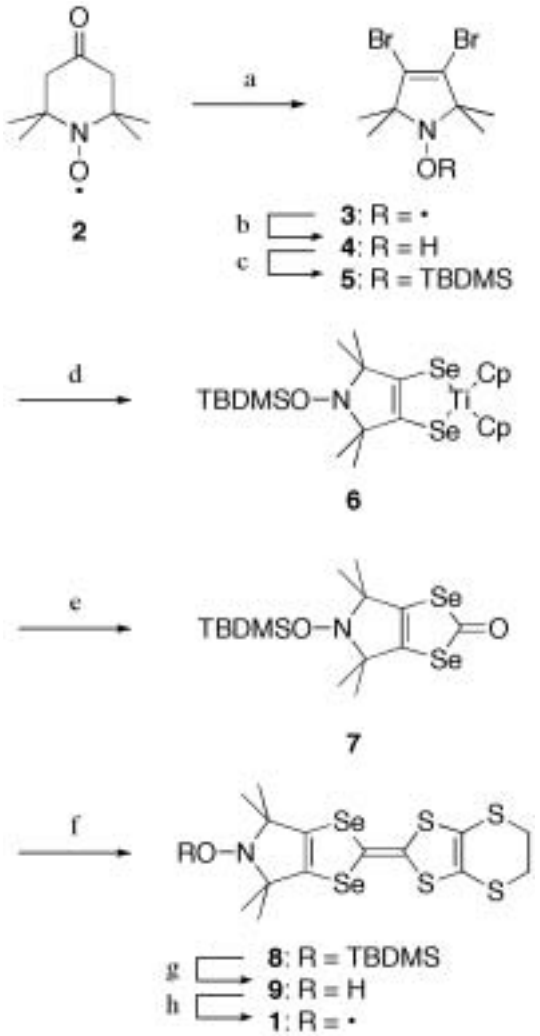


**Scheme 1.** Synthesis of PROXYL-ET.
(a) NaOBr; (b) Diphenylhydrazine; (c) TBDMSOTf; (d) t-BuLi, Se, $Cp_2TiCl_2$, THF; (e) triphosgene, THF; (f) 4,5-ethylenedithio-1,3-dithol-2-thione, $P(OMe)_3$, toluene; (g) TBAoF, THF; (h) $Ag_2O$, THF.

# IV-F Electronic and Magnetic Properties of π-Electron-Based Molecular Systems

π-electrons are an interesting building block in architecting functionalized electronic and magnetic molecular systems. We have focused on nano-sized graphite and TTF-based organic charge transfer complexes, in which π-electrons play an important role, in developing new types of molecular electronic systems. In nanographene, single layer nanographite, which is defined as flat open π-electron system have edges and contrasted to closed π-electron systems of fullerenes and carbon nanotubes, non-bonding π-electronic state appearing around the Fermi level generates unconventional nanomagnetism. We have found an interesting electronic wave interference effect in finite-sized graphite with distortion-network structures and anisotropy of the Raman spectra of nanographite ribbons. A combination of TTF-based π-electron donor and counteranion having localized spins is a useful way in producing molecular magnetic conductors, which are expected to have properties different from traditional metal magnets featured with s-d interaction. Under this scheme, we have developed a new class of TTF-based organic magnetic conductors. The interaction between the conducting π-electrons of donors and the localized d-electrons of magnetic anions are found to show interesting interplay between magnetism and electron transport.

## IV-F-1 Metal-Insulator Transition in Iodinated Amorphous Conducting Carbon Films

**KUMARU, Latha[1]; SUBRAMANYAM, S. V.[1]; ETO, Soichiro[2]; TAKAI, Kazuyuki[2]; ENOKI, Toshiaki**
*([1]Indian Inst. Sci.; [2]Tokyo Inst. Tech.)*

[*Carbon* **42**, 2133–2137 (2004)]

In this work, the effect of iodine incorporation on the electrical conductivity, magnetic susceptibility (χ) and magnetoresistance (MR) of amorphous conducting carbon (a-C) films has been discussed. Variation in conductivity of a-C films depends on the sample preparation conditions and iodine concentration. Evidence of metal–insulator (M–I) transition as a function of pyrolysis temperature is observed for iodinated (a-C:I) samples. The temperature dependent magnetic susceptibility of a-C:I sample shows a Curie behavior at low temperatures. The positive magnetoresistance is observed for all the samples irrespective of the conduction regimes. This is accounted by the electron–electron interaction in the a-C:I system.

## IV-F-2 Magnetic Resonance Study of Nanodiamonds

**SHAMES, Alexander I.[1]; PANICH, A. M.[1]; KEMPIŃSKI, W.[2]; BAIDAKOVA, M. V.[3,4]; OSIPOV, V. Yu.[3]; ENOKI, Toshiaki; VUL', A. Ya.[3]**
*([1]Ben-Guiron Univ. Negev.; [2]Polish Acad. Sci.; [3]Ioffe Phys.-Tech. Sci.; [4]Tokyo Inst. Tech.)*

[NATO Science Sries, D. M. Gruen, O. A. Shenderova, A. Ya. Vul', Eds., Springer; Dondrecht/Boston/London, pp.271 (2005)]

Magnetic resonance techniques, namely Electron Paramagnetic Resonance (EPR) and solid state Nuclear Magnetic Resonance (NMR), are powerful non-destructive tools for studying electron-nuclear and crystalline structure, inherent electronic and magnetic properties and transitions in carbon-based nanomaterials. EPR allows to control purity of ultradispersed diamond (UDO) samples, to study the origin, location and spin-lattice relaxation of radical-type carbon-inherited paramagnetic centers (RPC) as well as their transformation during the process of temperature driven diamond-to-graphite conversion. Solid state NMR on $^{1}H$ and $^{13}C$ nuclei provide one with information on the crystalline quality, allows quantitative estimation of the numbers of different allotropic forms, and reveals electron-nuclear interactions within the UDO samples under study. Results of recent EPR and $^{13}C$ NMR study of pure and transition metal doped UDD samples, obtained by detonation technique, are reported and discussed. In addition to characteristic EPR signals, originated from para- and ferromagnetic impurities and doping ions, the UDD samples show a high concentration of RPC (up to $10^{20}$ spin/gram), which are due to structural defects (dangling C–C bonds) on the diamond cluster surface. *In-situ* EPR sample's vacuumization experiment in conjunction with precise SQUID magnetization measurements allowed concluding that each UDD particle carries a single spin (dangling bond) per each from 8 crystal (111) facets bounded the particle.

## IV-F-3 *d*-Electron-Induced Negative Magnetroresistance of π-*d* Interaction System Including Brominated-TTF Donor

**NISHIJO, Junichi[1]; MIYAZAKI, Akira[1]; ENOKI, Toshiaki; WATANABE, Ryoji[2]; KUWATANI, Yoshiyuki[3]; IYODA, Masahiko[3]**
*([1]Indian Inst. Sci.; [2]Tokyo Inst. Tech.; [3]Tokyo Metropolitan Univ.)*

[*Inorg. Chem.* **44**, 2493–2506 (2005)]

A new π-d interaction system $(EDT\text{-}TTFBr_2)_2FeBr_4$ (EDT-TTFBr$_2$ = 4,5-dibromo-4',5'-ethylenedithiotetrathiafulvalene) and its nonmagnetic anion analogue $(EDT\text{-}TTFBr_2)_2GaBr_4$ based on a brominated TTF-type organic donor are investigated. The salts featured by quasi-1D π-electronic systems are metallic with metal-insulator transitions taking place at about 20 and 70 K for the $FeBr_4^-$ and $GaBr_4^-$ salts, respectively, where the low-temperature insulating state is associated with charge ordering or a Mott insulator followed by an antiferromagnetic transition at lower temperatures. The

$FeBr_4^-$ salt is featured with an antiferromagnetic transition of the anion d spins at a Néel temperature ($T_N$) = 11 K, which is significantly high despite its long anion-anion Br-Br contact, suggesting the importance of the π-d interaction in the magnetism. The surprisingly strong π-d interaction, *ca*. –22.3 K estimated from the magnetization curve, evidences the usefulness of the chemical modification of the donor molecule with bromine substitution to achieve strong intermolecular interaction. The antiferromagnetic state of the anion d spins affects the transport of the conducting π electrons through the strong π-d interaction, as evidenced by the presence of a resistivity anomaly of the $FeBr_4^-$ salt at $T_N$. Below $T_N$, the $FeBr_4^-$ salt shows negative magnetoresistance that reaches –23% at the highest magnetic field investigated ($B$ = 15 T), whereas only a small positive magnetoresistance is observed in the π-electron-only $GaBr_4^-$ salt. The mechanism of the negative magnetoresistance is explained by the stabilization of the insulating state of the π electrons by the periodic magnetic potential of the anion d spins in the $FeBr_4^-$ salt, which is modified by applying the external magnetic field.

### IV-F-4 Electronic and Mgnetic Properties of π-*d* Interaction System $(EDTDM)_2FeBr_4$

**OKABE, K.[1]; YAMAURA, J. -I.[2].; MIYAZAKI, Akira[1]; ENOKI, Toshiaki**
*([1]Tokyo Inst. Tech.; [2]Univ. Tokyo)*

[*J. Phys. Soc. Jpn.* **74**, 1508–1520 (2005)]

The crystal structure and electronic and magnetic properties of magnetic molecular conductor $(EDTDM)_2FeBr_4$ are investigated. The material undergoes a SDW transition at $T_{MI}$ ~ 11 K and an antiferromagnetic transition of $Fe^{3+}$ *d*-spins at $T_N$ = 3 K. In addition to the appearance of an anomaly in the resistivity around $T_N$, a large magnetoresistance is observed below $T_N$, which diverges at the critical pressure ($P_c$ ~ 9.2 kbar) of the MI transition. The perturbation potential from the antiferromagnetic $Fe^{3+}$ spin arrangement stabilizes the SDW state, leading to the anomaly in the resistivity. The application of magnetic field reduces the potential of the $Fe^{3+}$ spins, which leads to the large negative magnetoresistance. This indicates that the π-*d* interaction plays an important role in the interplay between the magnetism and the electron transport.

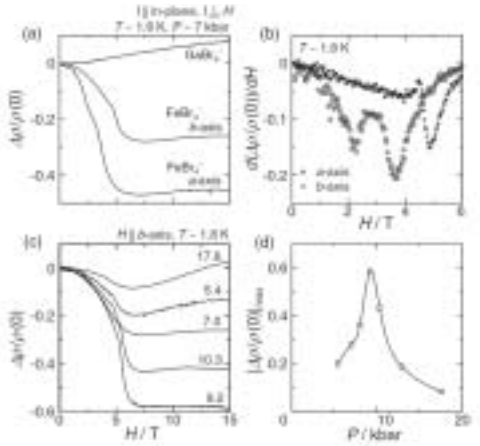


**Figure 1.** The field dependence of the magnetoresistance at $T$ ~ 1.9 K for $(EDTDM)_2MBr_4$ (M = Fe, Ga) under the pressure of 7.0 kbar. (b) The field dependence of the magnetoresistance at $T$ ~ 1.8 K for $(EDTDM)_2FeBr_4$ under pressures of 5.4, 7.0, 9.2, 10.3 and 17.6 kbar. (c) The numerical derivatives of the intra-layer magnetoresistance of $(EDTDM)_2FeBr_4$ at $P$ ~ 7.0 kbar as a function of applied field. (d) The pressure dependence of the maximum of the absolute value of the negative magnetoresistance of $(EDTDM)_2FeBr_4$.

### IV-F-5 Observation of Zigzag- and Armchair-Edges of Graphite

**KOBAYASHI, Yousuke[1]; KUSAKABE, Koichi[2]; FUKUI, Ken-ichi[1]; ENOKI, Toshiaki; KABURAGI, Yutaka[3]**
*([1]Tokyo Inst. Tech.; [2]Osaka Univ.; [3]Musashi Inst. Tech.)*

[*Phys. Rev. B* **71**, 193406 (4 pages) (2005)]

The presence of structure-dependent edge states of graphite is revealed by both ambient and ultra high vacuum (UHV) scanning tunneling microscopy and scanning tunneling spectroscopy observations. On a hydrogenated zigzag (armchair) edge, bright spots are (are not) observed together with a ($\sqrt{3}\times\sqrt{3}$) *R*30° superlattice near the Fermi level ($V_S$ ~ –30 mV for a peak of the local density of states) under UHV (Figure 1), demonstrating that a zigzag edge is responsible for the edge states, although there is no appreciable difference between as-prepared zigzag and armchair edges in air. Even in the hydrogenated armchair edge, however, bright spots are observed at defect points, at which partial zigzag edges are created in the armchair edge.

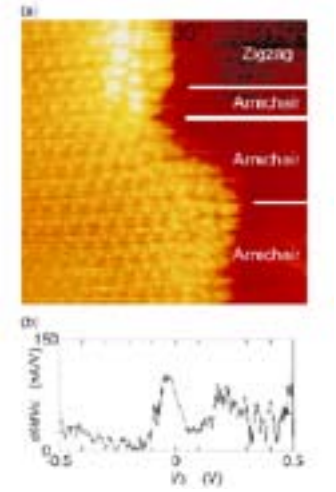


**Figure1.** (Color) (a) An atomically resolved UHV STM image of zigzag and armchair edges (9 × 9 $nm^2$). (b) Typical $dI/dV_S$ curve from STS data at a zigzag edge.

# IV-G Progress of Conjugated Phenomena Coupled with Spin and Photon for Assembled Hetero-Molecular System

Intercalation of photochromic molecule into magnetic system provides fascinating multi-functionalities such as photo-magnetism, which gains much attention for their application to devices. The main subjects in this project are the development of photo-induced spin-crossover phenomena at room temperature by using the photo-isomerization of intercalated molecule, and the development of the transformation of magnetism for two-dimensional ferromagnetic system coupled with photochromic molecule.

## IV-G-1 Reversible Photomagnetism in a Cobalt Layered Compound Coupled with Photo-Chromic Diarylethene

**OKUBO, Masashi[1]; ENOMOTO, Masaya[1]; KOJIMA, Norimichi[2]**
*([1]Univ. Tokyo; [2]IMS and Univ. Tokyo)*

[*Solid State Commun.* **135**, 777 (2005)]

Photomagnetism is one of the most attractive topics in recent research on molecular solids. In order to produce a photo-controllable magnet, we have synthesized a novel organic-inorganic hybrid system coupled with a photochromic diarylethene anion, 2,2'-dimethyl-3,3'-(perfluorocyclopentene-1,2-diyl)bis(benzo [b]thiophene-6-sulfonate)(**1a**) and cobalt LDHs (layered double hydroxides). The anion exchange reaction between the diarylethene anion, **1a**, and the layered double hydroxide, $Co_2(OH)_3(CH_3COO)\cdot H_2O$ (**2**), takes place successfully (Figure 1), which was elucidated by powder X-ray diffraction analysis and IR spectra. Based on the elemental analysis, the title compound synthesized by the anion exchange reaction between **2** and **1a** has the chemical composition, $Co_4(OH)_7(\mathbf{1a})_{0.5}\cdot H_2O$ (**3**). Powder X-ray diffraction analysis revealed the interlayer distance of $c$ = 27.8 Å. The magnetic susceptibility measurements elucidated the ferromagnetic intra- and inter-layer interactions and the Curie temperature of $T_c$ = 9 K.

In order to investigate the photo-irradiation effect on the magnetism, we carried out light irradiation on **3** spread thin on a glass plate in the dark at room temperature. After the irradiation, we measured the temperature dependence of the AC and DC susceptibilities and the hysteresis loop at 2 K. Although there is no light irradiation effect on the Curie temperature, the hysteresis loop shows a photomagnetic effect. The coercive field as well as the remnant magnetization decreases from 940 Gauss to 550 Gauss after light irradiation of 313 nm. The initial hard magnet is switched to a soft magnet by light irradiation of 313 nm. In addition, the soft magnet is almost reversibly returned to the initial hard magnet by the light irradiation of 550 nm. As plotted in Figure 2, both the coercive field and the remnant magnetization change almost reversibly by light irradiation of 313 nm and 550 nm. By UV irradiation of 313 nm, **3** shows the photo-isomerization of diarylethene anion from the open form to the closed one in solid state, which leads to the decreases in the coercive field and the remnant magnetization. Furthermore, the photo-excited state is returned to the initial state (open form) almost reversibly by visible-light irradiation of 550 nm. In this manner, we have succeeded in controlling the magnetic properties reversibly by two kinds of photo-irradiation for the organic-inorganic hybrid system, **3**.[1)]

**Reference**

1) M. Okubo, M. Enomoto and N. Kojima, *Solid State Commun.* **134**, 777–782 (2005).

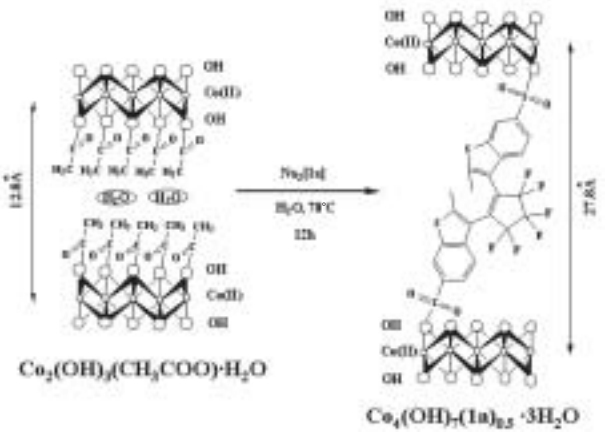


**Figure 1.** Schematic representation of the anion exchange reaction and the structure of **3**.

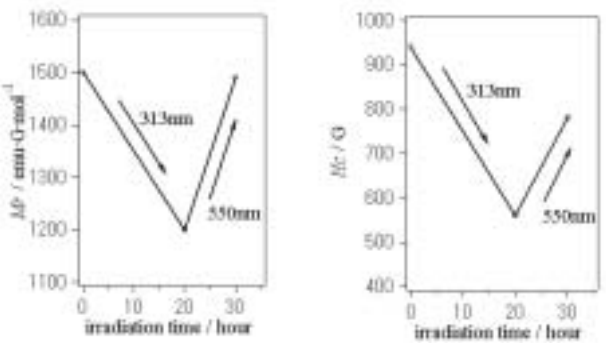


**Figure 2.** Photo-irradiation effects on the coercive field ($H_c$) and the remnant magnetization ($M_r$) of **3** at 2 K.

# IV-H Molecular Crystals toward Nano-Devices by Use of d-π Interaction, Crystal Designing and Optical Doping

After some 30 years' intensive research on molecular charge transfer (CT) salts as potential functional materials, the research field has now gotten ready to examine how to make them into actual devices. Such efforts are concentrated on the developments of organic thin films for field effect transistors and light-emitting devices, both of which are carried out in a number of laboratories and groups with worldwide competitions. In order to examine the potential applicability of molecular materials from a different point of view, we are carrying out basic studies on development and physical properties of molecular CT single crystals. Major part of our study can be classified into three categories; the physical properties of the CT salts including localized spins, crystal designing using polycarboxylate anions, and device formation by optical doping method.

## IV-H-1 Light-Induced Transformation of Molecular Materials into Devices

**NAITO, Toshio; INABE, Tamotsu[1]; NIIMI, Hironobu[1]; ASAKURA, Kiyotaka[1]**
*([1]Hokkaido Univ.)*

[*Adv. Mater.* **16**, 1786–1790 (2004)]

Many kinds of molecular solids are now attracting a worldwide interest as promising candidates for advanced materials such as electronic/magnetic/optical devices and energy converters. In particular, semiconductor diodes based on photovoltaic effect appear one of the most effective ways to utilize molecular materials, if there is an appropriate doping method available. This work concerns a finding of a novel method of (persistent) carrier doping to molecular materials. The method is simple and versatile; just illuminating the desired part of material as long as it contains a photosensitive chemical species in addition to an electroactive one. Although various kinds of photoexcited states reported thus far have typical lifetimes of some hundreds of micro-seconds at longest in general, the doped state survived even several months after the illumination was finished. The experimental results demonstrate that one can control the conducting properties of an arbitrary part of a molecular material using appropriately focussed illumination. In other words, this method opens a new way for making devices and conducting nano-architectures from a wide variety of molecular solids, which have awaited for a space-resolved doping method under a mild condition.

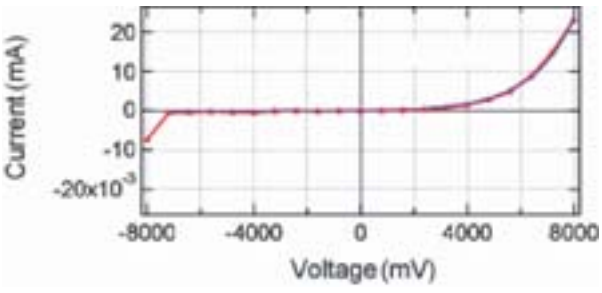


**Figure 1.** Current-Voltage property curve of the single crystal of $Ag(DM)_2$ after UV-VIS illumination upon only half of it for ~21 days.

## IV-H-2 Molecular Conductors Containing Photoreactive Species

**NAITO, Toshio; INABE, Tamotsu[1]**
*([1]Hokkaido Univ.)*

[*J. Phys. IV France* **114**, 553–555 (2004)]

In order to examine the possibility of (persistent) carrier doping to molecular crystals by light exposure, some different types of molecular crystals containing photoreactive species are synthesized and characterized. The $[Ru(bpy)_3]^{2+}$ cation (bpy = 2,2'-bipyridyl) yielded two different new complexes with $[Ni(dmit)_2]^-$ radical species, both of which were structurally characterized and turned out to be band insulators. Methy viologen (MV) has been found to yield a new phase of the complex with $[Ni(dmit)_2]^-$, $MV[Ni(dmit)_2]_2$. The temperature dependences of electrical resistivity (decreasing with lowering temperature down to 1.0 K) and magnetic susceptibility (Pauli paramagnetism from 300 K to 1.8 K with a hysteresis below ~100 K) clearly indicate that this phase is metallic. The thermoelectric power exhibited ~0 $\mu VK^{-1}$ from 300 K–4.2 K. This phase turned out to be metastable, and the crystals gradually turned into insulating ones. The effects of UV-VIS light exposure to the conducting and magnetic properties of Ag(DMe-DCNQI)$_2$ have been studied, and clear differences between the exposed and the pristine crystals were observed. The ESR signal at 3.7 K suggested that the exposed sample should include the Ag(0) species.

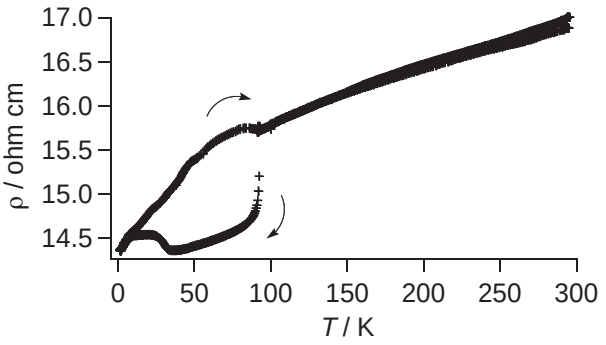


**Figure 1.** Temperature-dependent electrical resistivity of $MV[Ni(dmit)_2]_2$.

## IV-H-3 A New Optical Doping Method toward Molecular Electronics

**NAITO, Toshio; INABE, Tamotsu[1]; NIIMI, Hironobu[1]; ASAKURA, Kiyotaka[1]**
*([1]Hokkaido Univ.)*

[*Synth. Met.* **152**, 289–292 (2005)]

This work concerns a finding of a novel method of (persistent) carrier doping to molecular materials. The method is simple and versatile; just illuminating the material as long as it contains a photosensitive chemical species in addition to an electroactive one. Although various kinds of photo-excited states reported thus far have typical lifetimes of some hundreds of microseconds at longest in general, the doped state survived even a week after the illumination was finished. The experimental results demonstrate that one can control the conducting properties of an arbitrary part of a molecular material using appropriately focussed illumination. In other words, this method opens a new way for making devices and conducting nano-architectures from a wide variety of molecular solids, which have awaited for a space-resolved doping method.

## IV-H-4 Photochemical Method of Device Fabrication Starting from Molecular Crystals

**NAITO, Toshio; SUGAWARA, Hideyuki[1]; INABE, Tamotsu[1]; MIYAMOTO, Takeshi[1]; NIIMI, Hironobu[1]; ASAKURA, Kiyotaka[1]**
*([1]Hokkaido Univ.)*

[*Mol. Cryst. Liq. Cryst.* submitted]

The conductivity of a silver salt of *N*,*N*'-dicyanoquinonediimine irreversibly varied in approximate proportion to an illumination of a wide range of wavelengths. Depending on the illumination conditions, four different states (β, γ, δ, and ε) were obtained with different structures. The β structure is in particular important, where the formal charge of the *N*,*N*'-dicyanoquinonediimine molecules continuously decreased to –0.4– –0.35 with retaining the crystal structure, when we kept the temperature < 155 ºC during the illumination. The non-illuminated area of the sample retained its original electrical property with a well-defined interface, which enabled a fabrication of a junction-structure in the single crystal.

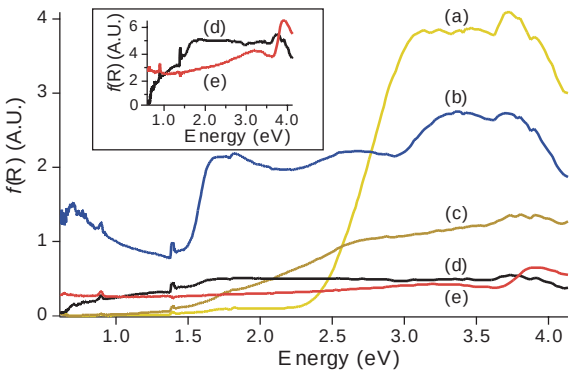


**Figure 1.** Diffuse scattering spectra of (a) isolated neutral DM species, (b) α-, (c) γ-, (d) δ-, and (e) ε-$Ag(DM)_2$, respectively. The inset shows (d) and (e) spectra with $f(R)$ enlarged by 10 times.

## IV-H-5 Photochemical Control of Dark Conductivity—A New Approach to Devices Based on Molecular Crystals

**NAITO, Toshio; SUGAWARA, Hideyuki[1]; INABE, Tamotsu[1]; KITAJIMA, Yoshinori[2]; MIYAMOTO, Takeshi[1]; NIIMI, Hironobu[1]; ASAKURA, Kiyotaka[1]**
*([1]Hokkaido Univ.; [2]KEK)*

[*J. Low Temp. Phys.* submitted]

Thermal analysis of $Ag(DM)_2$, where DM = 2,5-dimethyl-*N*,*N*'-dicyanoquinonediimine, clarified that the salt had an insulating amorphous phase (≥ 155 °C). Characterization of this and related solid states of $Ag(DM)_2$ indicated that a photo-induced process should be essential in controlling the number of carriers and thus conduction behavior of the salt by illumination. In fact, while heating could do nothing but make the salt insulating when the sample temperature exceeded 155 °C, ultraviolet-visible light illumination (< 155 °C) could gradually change the properties to be semiconducting with retaining the crystal lattice (average structure).

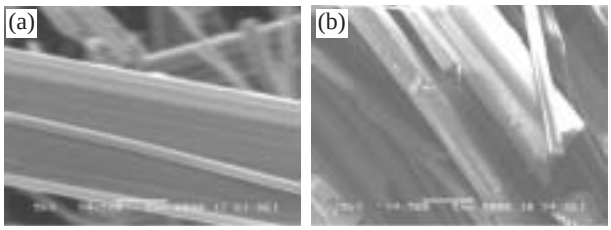


**Figure 1.** Scanning Electron Microprobe (SEM) photographs of different states after UV-Vis illumination on single crystals of $Ag(DM)_2$; (a) β-, and (b) γ-states, respectively. The SEM photographs of the pristine (α-) samples (not shown here) much resemble those of the β-state.

## IV-H-6 Molecular Unit Based on Metal Phthalocyanine; Designed for Molecular Electronics

**MATSUDA, Masaki[1]; HANASAKI, Noriaki[1]; IKEDA, Shingo[1]; TAJIMA, Hiroyuki[1]; NAITO, Toshio; INABE, Tamotsu[2]**
*([1]Univ. Tokyo; [2]Hokkaido Univ.)*

[*J. Phys. IV France* **114**, 541–543 (2004)]

We obtained three conducting crystals based on a $[Fe^{III}(Pc)(CN)_2]$ molecular unit. All crystals showed a large anisotropic negative magnetoresistance arising from the π-d interaction self-contained in the $[Fe^{III}(Pc)(CN)_2]$ unit. The anisotropy is attributable to the anisotropic *g*-tensor in the $[Fe^{III}(Pc)(CN)_2]$ unit. We also obtained a thin film containing $[Fe^{II}(Pc)(CN)_2]$. The film exhibits photocurrent response for the UV irradiation. These features suggest $[M(Pc)(CN)_2]$ molecular

unit is a well-designed one for a building block of molecular devices.

### IV-H-7 Anisotropic Giant Magnetoresistance Originating from the π-d Interaction in a Molecule

**MATSUDA, Masaki[1]; HANASAKI, Noriaki[1]; TAJIMA, Hiroyuki[1]; NAITO, Toshio; INABE, Tamotsu[2]**
*([1]Univ. Tokyo; [2]Hokkaido Univ.)*

[*J. Phys. Chem. Solids* **65**, 749–752 (2004)]

We synthesized TPP[$Fe^{III}$(Pc)$(CN)_2]_2$, $PTMA_x$[$Fe^{III}$(Pc)$(CN)_2$]·*y*(MeCN), and PXX[$Fe^{III}$(Pc)$(CN)_2$], a new series of charge-transfer salts containing the axially-substituted phthalocyanine (Pc), [$Fe^{III}$(Pc)$(CN)_2]^-$. In this molecular unit, the π conduction electron derived from the Pc-ring coexists with the d electron which is a potential source of a local magnetic moment. Therefore various phenomena associated with the interplay between local magnetic moments and conduction electrons are expected. We observed the giant negative magnetoresistance (GNMR) in all the three salts. The GNMR is highly anisotropic for the magnetic-field direction, and reflects the *g*-tensor anisotropy of the local magnetic moment in the [$Fe^{III}$ (Pc)$(CN)_2]^-$ unit. This indicates that the GNMR in these salts originates from the strong π-d interaction in the [$Fe^{III}$(Pc)$(CN)_2]^-$ unit.

### IV-H-8 Phthalocyanine-Pphthalocyanine Salt Crystal: A Unique Assembly Design

**OHTSUKA, Yoshikazu[1]; NAITO, Toshio; INABE, Tamotsu[1]**
*([1]Hokkaido Univ.)*

[*J. Porphyrins Phthalocyanines* **9**, 68–71 (2005)]

A unique salt composed of cationic and anionic phthalocyanine complexes has been prepared and structurally characterized. The cationic component is di(pyridine)(phthalocyaninato)cobalt(III) and the anionic one is dicyano(phthalocyaninato)cobalt(III). They arrange alternately in the crystal, forming a two-dimensional sheet with partial π-π overlaps.

### IV-H-9 Physical Properties of Electrically Conducting and Stable Molecular Neutral Radical Solid [Co(2,3-Nc)$(CN)_2$]$CH_3CN$ (2,3-Nc = 2,3-Naphthalocyanine)

**NAITO, Toshio; MATSUMURA, Naoko[1]; INABE, Tamotsu[1]; MATSUDA, Masaki[2]; TAJIMA, Hiroyuki[2]**
*([1]Hokkaido Univ.; [2]Univ. Tokyo)*

[*J. Porphyrins Phthalocyanines* **8**, 1258–1268 (2004)]

Solid state properties of dicyano(2,3-naphthalocyaninato)cobalt(III) neutral radical crystal, [Co(2,3-Nc)$(CN)_2$]$CH_3CN$, were characterized by the measurements of the resistivity under high pressure and under uniaxial strain, thermoelectric power, magnetic susceptibility, ESR and polarized reflectance spectra. The title compound exhibited thermally activated-type electrical conductivity along the *c*-axis. The room temperature (RT) resistivity $\rho_{RT}$ along the *c*-axis and activation energy $E_a$ rapidly decreased with increasing pressure. The temperature-dependent thermoelectric power *S* was that of a typical one-dimensional (1D) semiconductor. However the high absolute value of *S* suggested that this electronic system should be strongly correlated. Although the electrical resistivity exhibited monotonical temeperature-dependence, the magnetic susceptibility clearly indicated a Peierls-type transition and marked fluctuation from RT. Both of Peierls-type transitions and fluctuations are characteristic phenomena to 1D conductors. Furthermore ESR spectra manifested that the Peierls-type transition occurred at 100 K. The inconsistency between the electrical behaviour (without a phase-transition) and magnetic behaviour (with a phase-transition) indicates the separation of the degrees of freedom in spin and charge (spin-charge separation) of this material. Spin-charge separation is a theoretically predicted phenomenon peculiar to the 1D conductors with strong correlation. The reflectance spectra were quantitatively explained by a 1D Hubbard model, and manifested the existence of a structural fluctuation of this material from RT. Based on these observed physical properties it is concluded that [Co(2,3-Nc)$(CN)_2$]-$CH_3CN$ is a strongly correlated 1D semiconductor with a Mott-Hubbard type energy gap and characterised with a fluctuation and spin-charge separation.

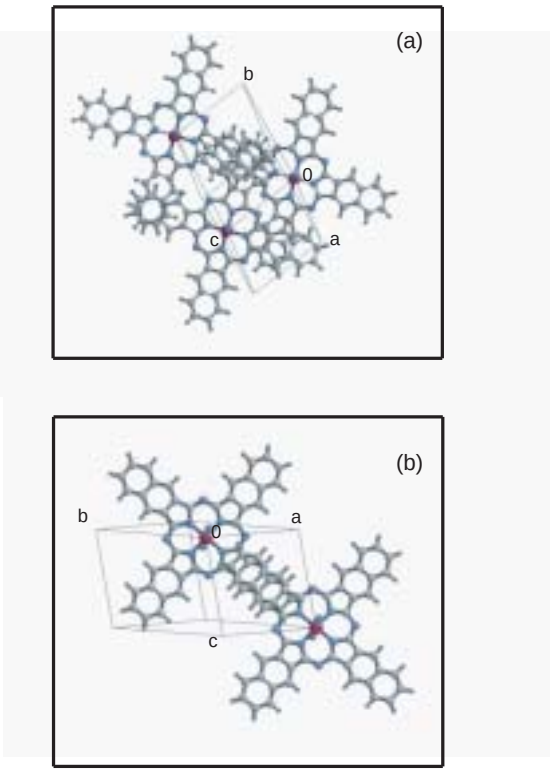


**Figure 1.** Crystal structure. For simplicity, (a) only three radical species at origin, [011] and [001], and (b) two radical species at origin and [101] are shown. The $CH_3CN$ molecules are omitted for clarity.

## IV-H-10 Charge Disproportionation and Anomalous Giant Magnetoresistance in a One-dimensional Conductor, TPP[Co(Pc)(CN)$_2$]$_2$

**TAJIMA, Hiroyuki[1]; HANASAKI, Noriaki[1]; MASUDA, Kouki[1]; MATSUDA, Masaki[1]; KODAMA, Katsuaki[1]; TAKIGAWA, Masashi[1]; OHMICHI, Eiji[1]; OSADA, Toshihito[1]; NAITO, Toshio; INABE, Tamotsu[2]; HASEGAWA, Hiroyuki[3]**
*([1]Univ. Tokyo; [2]Hokkaido Univ.; [3]NICT)*

[*Synth. Met.* in press]

Magnetoresistance study on the charge transfer salts of [Fe(Pc)(CN)$_2$] revealed various interesting phenomena, such as anisotropic giant negative magnetoresistance, weak ferromagnetism, and anisotropic Curie-Weiss magnetic susceptivility.[1)] These interesting phenomena originate from the orbital magnetic moment remaining in the [Fe(Pc)(CN)$_2$] unit, and the d-π interaction inherently existing in this unit. Contrary to the [Fe(Pc)(CN)$_2$] salts, physical properties of the [Co(Pc)(CN)$_2$] salts have not been investigated in detail. In this paper, we report the magnetotransport and NQR studies on TPP[Co(Pc)(CN)$_2$]$_2$ salts. This salt is a one-dimensional conductor, where the partially oxidized [Co(Pc)(CN)$_2$] units stack uniformly along the *c*-axis. The salt exhibits Pauli-paramagnetic susceptibility. The electrical resistivity is semiconducting with a very small activation energy less than 0.01 eV. Interestingly, this salt exhibits very large positive magnetoresistance at low-temperature ($\Delta R$(8 T)/$R$(0 T) ~ 6). Moreover, the field orientation dependence is quite small below 10 T. These facts indicate that the magnetoresistance in this salt is not an ordinary orbital effect. In order to examine the mechanism of the anomalous magnetoresistance, we have measured $^{59}$Co NQR spectra. We found a sign of charge disproportionation at 1.8 K. On the basis of magnetotransport ($B$ < 38 T), NQR and NMR ($B$ < 16 T) measurements, we will discuss the anomalous electronic state of this salt.

**Reference**

1) For example see, N. Hanasaki *et al.*, *Phys. Rev. B* **62**, 5839–5842 (2000).

## IV-H-11 Structural, Electrical and Magnetic Properties of α-(ET)$_7$[MnCl$_4$]$_2$·(1,1,2-C$_2$H$_3$Cl$_3$)$_2$ (ET = bis(ethylenedithio)tetrathiafulvalene)

**NAITO, Toshio; INABE, Tamotsu[1]**
*([1]Hokkaido Univ.)*

[*Bull. Chem. Soc. Jpn.* **77**, 1987–1995 (2004)]

A new charge-transfer salt of ET with a chloromanganate(II) complex anion has been synthesized and characterized by X-ray structural analysis, resistivity measurements, magnetic susceptibility, electron spin resonance (ESR) and extended Hückel tight biding band calculation. The crystal has a sheet structure comprised of α-type two-dimensional (2D) donor arrangement in the *bc*-plane and insulating sheets of discrete [MnCl$_4$]$^{2-}$ anions and 1,1,2-C$_2$H$_3$Cl$_3$ (TCE) molecules. Its conducting property exhibits considerable anisotropy, which is of effectively metallic along the *b*-axis down to 1.2 K under 2.9 kbar and higher pressure. The magnetic susceptibility is approximately reproduced by the Curie-Weiss law with the Weiss temperature θ = –(1.35±0.07) K from 2–300 K. ESR measurements revealed that the π-electron system in this salt exhibits Pauli paramagnetism at least at 3.6– ~50 K. The band calculation suggests that the HOMO (the highest occupied molecular orbital) band has extremely small dispersion almost solely along the *b**-axis with a simple one-dimensional (1D) Fermi surface. Considering all the data above, it is concluded that this salt has unusually stable and narrow 1D metallic band structure, which is a rare example even in a great number of molecular conducting salts reported to date.

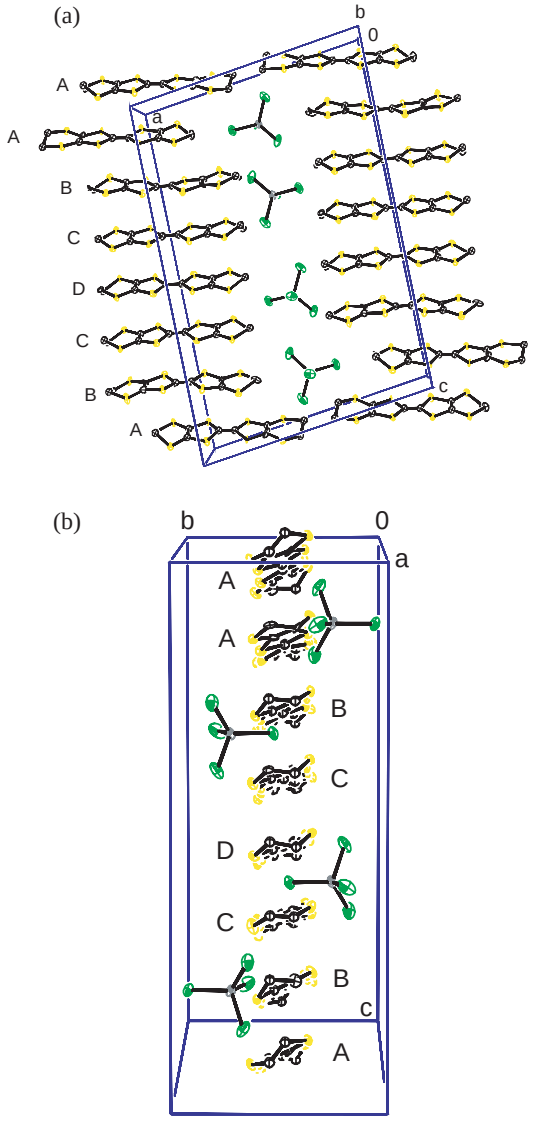


**Figure 1.** Unit cell; front view of (a) *ac*-, and (b) *bc*-planes. Hydrogen atoms are omitted for clarity.

## IV-H-12 New Binuclear Copper Complexes [(9S3)Cu(CN)Cu(9S3)]X$_n$ (X = BF$_4$, *n* = 1; X = TCNQ, *n* = 2) (9S3 = 1,4,7-trithiacyclononane): Syntheses, Crystal Structures and Magnetic Properties

**NAITO, Toshio; NISHIBE, Kunimasa[1]; INABE, Tamotsu[1]**
*([1]Hokkaido Univ.)*

[*Z. Anorg. Allg. Chem.* **630**, 2725–2730 (2004)]

The binuclear Cu complexes of 1,4,7-trithiacyclononane (9S3) with an inorganic anion ($BF_4^-$) and with an organic radical anion $TCNQ^-$ (7,7',8,8'-tetracyanoquinodimethanide) were synthesized and their molecular and crystal structures were examined in connection with each magnetic property. A new complex cation [Cu(9S3)CN(9S3)Cu] varied its charges and magnetic properties depending on the counter anions; [Cu(9S3)-CN(9S3)Cu]($BF_4$) (**1**) was obtained as diamagnetic colorless crystals, while [Cu(9S3)CN(9S3)Cu]$(TCNQ)_2$ (**2**) was obtained as dark blue crystals with antiferromagnetic property. Complex **1** crystallized in the monoclinic space group *C*2/c with $a$ = 26.863(2), $b$ = 7.0878(5), $c$ = 13.4864(8) Å, β = 116.318(2)°. Complex **2** crystallized in the triclinic space group $P\bar{1}$ with $a$ = 12.521(1), $b$ = 20.2698(8), $c$ = 8.0205(4) Å, α= 100.688(4), β = 93.846(5), γ = 94.953(4)°. Both complexes were comprised of cyano-bridged two Cu(9S3) ions with tetrahedral coordination geometry. The X-ray structural study revealed that **1** had two crystallographically equivalent Cu(I) centers, while **2** had two crystallographically independent Cu(I/II) sites. The two Cu(I/II) sites could not be distinguished from the X-ray structural study. As for **2** the IR spectra showed that both crystallographically independent TCNQ species were monoanions and were strongly dimerized due to pstacking, which well explained their diamagnetic contribution to the magnetic susceptibility and the highly insulating property of this salt. The temperature-dependent magnetic susceptibility of **2** showed a deviation from the Curie-Weiss behavior around 60 K, which indicated a strong antiferromagnetic intermolecular interaction between the copper complexes and that such intermolecular interaction should partly occur *via* the TCNQ radical anion dimer.

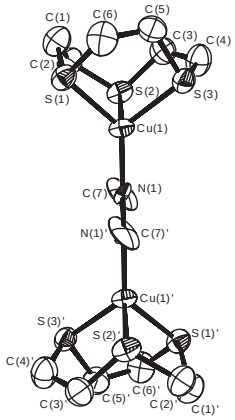


**Figure 1.** The molecular structure of the [Cu(9S3)CN(9S3)-Cu]$^+$ cation (50% probability ellipsoids). The hydrogen atoms are omitted for clarity.

## IV-H-13 Crystal Design of Cation-Radical Salts Based on the Supramolecular Self-Organizing Arrangement of Mellitate Anions

**INABE, Tamotsu[1]; KOBAYASHI, Norihito[1]; NAITO, Toshio**
*([1]Hokkaido Univ.)*

[*J. Phys. IV France* **114**, 449–453 (2004)]

Mellitate anions form hydrogen-bonding infinite networks in the salts with pyridinium cations. The network pattern depends on the number of deprotonation ($n$) from the mellitic acid; for $n$ = 3, triangular hydrogen-bond units form a two-dimensional sheet, while for $n$ = 2, dual hydrogen-bond units induce one-dimensional belts or two-dimensional grids. These self-organizing properties have been utilized for the crystal design of the TTF-type radical cation salts. Crystallization with TMTTF gave two kinds of crystals. One of the radical cation salt crystals consists of channel network of the anions and one-dimensional columns of TMTTF in the channels. In the other TMTTF salt, the anions with $n$ = 1 form a two-dimensional sheet with methanol molecules. The TMTTF radicals are packed between the sheets with their molecular planes parallel to the anion planes.

## IV-H-14 A Helical π-Radical Cation Column in the Double Helix of Mellitate Anions

**KOBAYASHI, Norihito[1]; NAITO, Toshio; INABE, Tamotsu[1]**
*([1]Hokkaido Univ.)*

[*Adv. Mater.* **16**, 1803–1806 (2004)]

Recent investigations of supramolecular network formation of mellitate anions in pyridinium salts have revealed that strong hydrogen bonds between the carboxy and carboxylate groups (the pair can be considered as dual hydrogen bond) predominantly form between neighboring anions, and its infinite sequence results in a chain, grid, or channel network. This self-organizing property is useful for aligning the cationic counterions. Herein, these anion structures have been utilized for the crystallization of π-radical cations. Electrochemical oxidation of TTF in the presence of mellitic acid and pyridine gave hexagonal platelets of $[TTF]_2[C_6(COO)_6H_4^{2-}]$. A TTF π-radical cation salt with a unique helical columnar structure has been successfully constructed within the supramolecular double helix of mellitate anions. The TTF radical tends to dimerize in a one-dimensional column; however, the twisting distortion induces a kink defect, which appears as orientational disorder. The absence of three-dimensionally correlated dimerization phase locking may arise from shielding of the one-dimensional column by the mellitate anions. This investigation indicates that combining charged functional molecules with a supramolecular network formed by their counterions is a promising approach to the crystal design of novel functional molecular materials. Indeed, it has recently been revealed that unique π-radical arrangements occurred in mellitate salts formed with other TTF-type molecules, in which mellitate anions formed a channel or sheet network by self-organization.

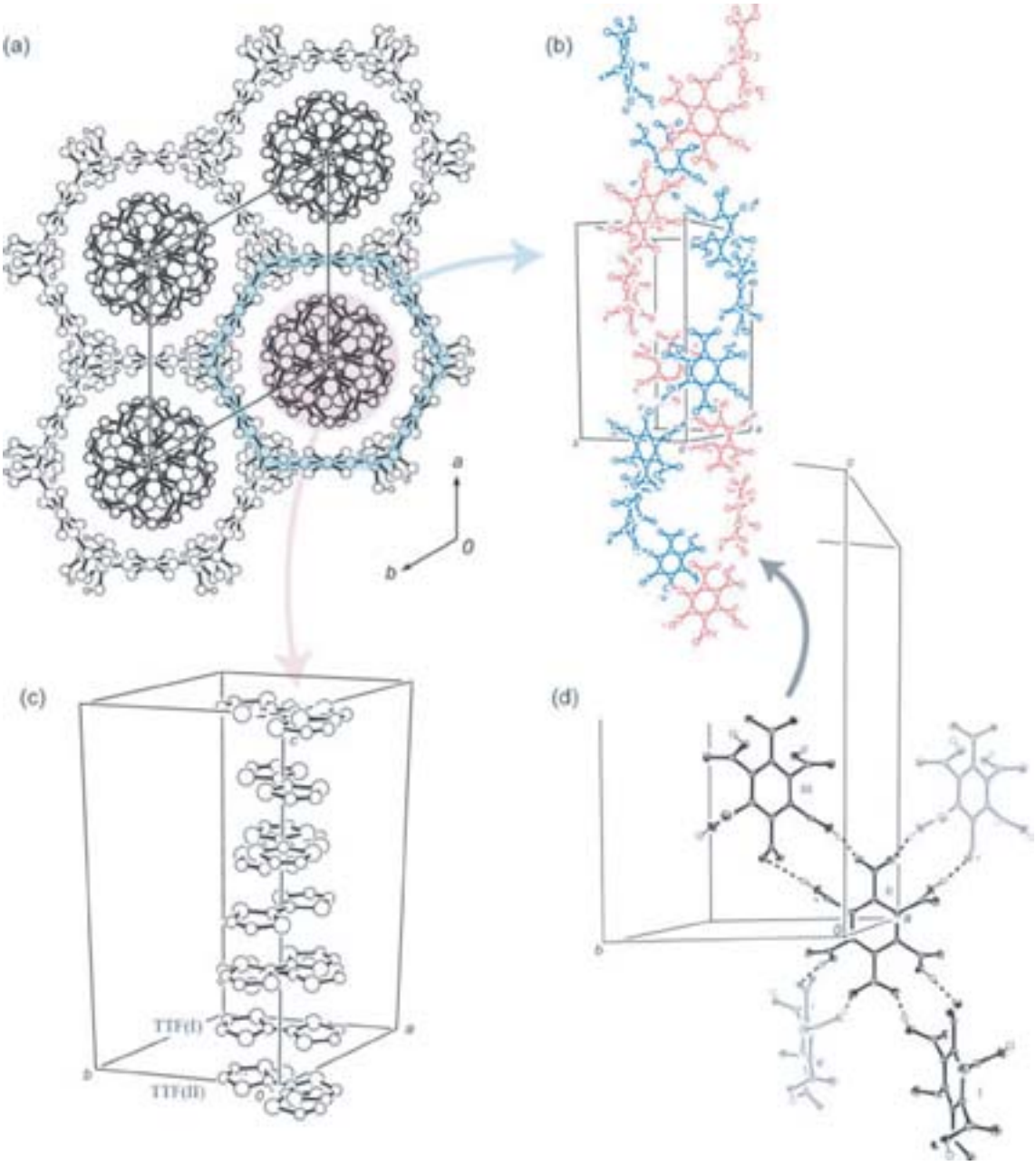


**Figure 1.** Molecular arrangement in $[TTF^{+}]_2[C_6(COO)_6H_4^{2-}]$. a) Hexagonal channel structure of mellitate anions and the TTF columns viewed along the *c*-axis. b) Mellitate-anion double helix. c) Helical TTF column. d) Hydrogen bond in the mellitate network; anions **I**, **II**, and **III** are related by the $6_2$ screw axis at (0,0,*z*).

### IV-H-15 Network Formation of Mellitate Anions ($[C_6(COO)_6H_{6-n}]^{n-}$) in the Salts with Piperidinium Derivatives and *o*-Phenylenediammonium

**KOBAYASHI, Norihito[1]; INABE, Tamotsu[1]; NAITO, Toshio**
*([1]Hokkaido Univ.)*

[*CrystEngComm* **6**, 189–196 (2004)]

Single crystals of mellitate anion ($[C_6(COO)_6H_{6-n}]^{n-}$) with piperidinium $[C_5H_{10}NH_2^{+}]_3[C_6(COO)_6H_3^{3-}]$ (**1**) and $[C_5H_{10}NH_2^{+}]_2[C_6(COO)_6H_4^{2-}]\cdot CH_3OH\cdot 3H_2O$ (**2**), with 1-methylpiperidinium $[C_5H_{10}NHCH_3^{+}]_2[C_6(COO)_6H_4^{2-}]\cdot 2H_2O$ (**3**), and with *o*-phenylenediammonium $[C_6H_4(NH_3)_2^{2+}]_2[C_6(COO)_6H_2^{4+}]\cdot 2CH_3OH$ (**4**) have been prepared and structurally characterized. In all of the salts, two-dimensional (2D) networks of mellitate anions were formed due to the strong self-organization of the anion. In **1**, a 2D hexagon-type network of hydrogen-bond has been observed to form among the anions. This is characteristic of the mellitate anions with $n = 3$ (*n*: deprotonation number from the acid). In other salts, a 2D anion network containing either water molecules or $-NH_3$ groups commonly formed. Since the network pattern occurs with different cation species, this hydrogen-bonding unit was determined to be dominant in the $n = 2$ anion with water and the $n = 4$ anion with $-NH_3$ species.

# IV-I Charge and Spin Dynamics of Organic Conductors

The spin and charge dynamics in organic conductors play important role in the emergence of the exotic properties in organic conductors, for example, superconductivity, magnetic ordering and charge ordering. It is important to reveal not only magnetic properties, but also the total picture of organic conductors. As known well, $^{13}$C-NMR is a one of the most powerful tool in the point of the magnetism. Since nuclear magnetic moment, *I*, is 1/2, $^{13}$C-NMR is not sensitive to the charge properties. On the other hand, optical studies, which are sensitive to the charge properties, are complementary to NMR study. In order to study both magnetic and charge properties, we performed $^{13}$C-NMR and optical works.

## IV-I-1 Electron Delocalization on κ-(BEDT-TTF)$_2$Cu$_2$(CN)$_3$ under Pressure

**KAWAMOTO, Atsushi[1]; HONMA, Yosuke[2]; KUMAGAI, Ken-ichi[2]; MATSUNAGA, Noriaki[2]; NOMURA, Kazushige[2]**
*([1]IMS and Hokkaido Univ.; [2]Hokkaido Univ.)*

[*Phys. Rev. B* submitted]

κ-(BEDT-TTF)$_2$X is a system, whose bandwidth is comparable to the effective onsite coulomb repulsion. The phase diagram of this system has been considered to represent the competition between anti-ferromagnetic insulating behavior and superconductivity.

The κ-(BEDT-TTF)$_2$X system have been well explained using a parameter, *U*/*W* as well as the high $T_c$ cuprates. Although κ-(BEDT-TTF)$_2$Cu$_2$(CN)$_3$ exhibited the superconductivity under pressure, this salt behaves as an insulator without magnetic ordering under ambient pressure. Similar to the case of other salts, AF fluctuations intensified with a decrease in temperature. In addition to that, line broadenings, which suggested inhomogeneous electron localization, was observed.

We have proposed that the electron localization effect is significant in a relatively narrow bandwidth of the salt and the scenario in which, pressure application increases the bandwidth, suppresses the localization and produces the superconductivity.

In order to determine the relationship between the insulator phase and the superconductivity and confirm the proposed scenario, we measured the $^{13}$C-NMR of κ-(BEDT-TTF)$_2$Cu$_2$(CN)$_3$ under pressures. We observed a decrease in the spin susceptibility with an increase in pressure and the suppression of the line broadening above critical pressure.

The temperature dependences of $(T_1T)^{-1}$ under pressures exhibited the same behavior as that of κ-(BEDT-TTF)$_2$X, where X = Cu[N(CN)$_2$]Br and Cu(NCS)$_2$.

These results suggested that the electronic structure of κ-(BEDT-TTF)$_2$Cu$_2$(CN)$_3$ under pressures is same as that of other κ-(BEDT-TTF)$_2$X salts. Moreover, they supported our scenario of the emergence of the superconductivity.

## IV-I-2 Coherent-Incoherent Crossover Behavior of Electron on κ-(BEDT-TTF)$_2$Ag(CN)$_2$·H$_2$O

**KAWAMOTO, Atsushi[1]; KUMAGAI, Ken-ichi[2]; YAMAMOTO, Kaoru; YAKUSHI, Kyuya**
*([1]IMS and Hokkaido Univ.; [2]Hokkaido Univ.)*

[to be submitted]

κ-(BEDT-TTF)$_2$X system showed the variety electronic states, for example, superconductivity (SC), anti-ferromagnetic ordering (AF), *etc.* Experimentally, the most impressive aspects are an adjustment between the superconducting and the magnetic ordering state and the peak of $(T_1T)^{-1}$ at $T^*$ in NMR study as observed in high $T_c$ cuprates. These result suggests the mechanism of superconductivity intermediated by magnetic fluctuations as same as high Tc cuprates. $^{13}$C-NMR is a one of the most powerful tool in the point of magnetic dynamics. On the other hand, optical studies, which are sensitive to the charge dynamics, are complementary to NMR study which detects the magnetism. We performed single crystal $^{13}$C-NMR and optical works. Many researchers paid the attention to mainly $T_c$ = 10 K class samples near the AF-SC boundary. However κ-(BEDT-TTF)$_2$Ag(CN)$_2$·H$_2$O, which is far from the boundary, should be paid the attention. Is there the peak structure in $(T_1T)^{-1}$ in this sample and the relationship between $T^*$ and SC?

We measured $^{13}$C-NMR and reflection spectrum in κ-(BEDT-TTF)$_2$Ag(CN)$_2$·H$_2$O. We could not observed the increase of the AF magnetic fluctuation as in κ-(BEDT-TTF)$_2$Cu[N(CN)$_2$]Cl. Results of $^{13}$C-NMR suggested the emergence of superconductivity did not require the increase of the AF magnetic fluctuation but the crossover to the Fermi liquid regime. Optical studies suggested the crossover corresponds to the development of the coherency of conduction electron.

## IV-I-3 Charge Ordering State on (BEDT-TTF)$_3$Cl$_2$·2H$_2$O

**KAWAMOTO, Atsushi[1]; OGURA, Takashi[2]; KUMAGAI, Ken-ichi[2]; TANIGUCHI, Hiromi[3]**
*([1]IMS and Hokkaido Univ.; [2]Hokkaido Univ.; [3]Saitama Univ.)*

[to be submitted]

The organic superconductors, as represented by κ-(BEDT-TTF)$_2$X, are attractive compound, because of the relationship between anti-ferromagnetic fluctuation and superconductivity well as High-$T_c$ cuprates. Since these κ-type salts are well known to have the nature of the strong dimerization, they can be considered as a half-filled electron system. Many experiments on κ-

$(BEDT\text{-}TTF)_2X$ have been well explained by the universal phase diagram using a parameter, $U/W$, where $U$ is the effective on-site coulomb repulsive energy and $W$ is the bandwidth.

On the other hand, if the dimerization is weak and the $U$ is small, the system cannot be regarded as half-filled system. In addition to the $U$, the effective off-site Coulomb repulsive energy $V$ makes the system form Charge Ordering (CO) state.

In some of organic conductors, such as α-type, θ-type salts, their insulator phase was said not to be antiferromagnetic ordering state. Since the dimerization in these salts is not so strong, the insulator phase of these salts is likely to form the CO state. Applying pressure, some of these salts show the superconductivity. Therefore we are also interested in the relationship between charge fluctuation and superconductivity. Quasi-two-dimensional (Q2D) organic conductor $(BEDT\text{-}TTF)_3Cl_2\cdot 2H_2O$ is metallic at 300 K and it undergoes metal-insulator transition (MIT) at $T \sim 150$ K from magnetic susceptibility and electric conductivity measurements. The MIT has been believed to be connected with charge density wave (CDW) formation. However, the formation of the charge ordering (CO) in the insulator phase was also expected. Using $^{13}$C-NMR measurement, we observed the split of the NMR spectrum which corresponded to the charge rich and poor sites below the MIT temperature and could conclude the insulator state is the CO state.